Journal of Forestry Research (2026) 37:146
https://doi.org/10.1007/s11676-026-02082-3

ORIGINAL PAPER

Ectomycorrhizal fungi redirect soil carbon stabilization pathways under nitrogen enrichment by regulating microbial necromass formation

Wenyuan He[1] · Yu Zhang[1] · Hongjian Wei[1] · Tingying Xu[2] · Wentao Hu[1] · Hui Chen[1] · Ming Tang[1]

Received: 19 January 2026 / Accepted: 30 March 2026
© The Author(s) 2026

Abstract Atmospheric nitrogen (N) deposition is altering forest soil carbon dynamics, yet the role of ectomycorrhizal (ECM) symbiosis in regulating soil organic carbon (SOC) stabilization under elevated N remains poorly understood. We investigated how N addition (0, 5, 10 and 20 mM urea) and ECM colonization interact to influence SOC partitioning, microbial functioning, and stabilization mechanisms in *Eucalyptus grandis* × *Eucalyptus urophylla* soils. ECM colonization remained consistently high across the N gradient, but fungal biomass declined with increasing N, indicating shifts in fungal allocation strategies. N addition alone favored accumulation of transient particulate organic carbon, whereas ECM inoculation promoted mineral-associated organic carbon (MAOC) at intermediate N levels, despite reductions in SOC hydrophobicity and chemical recalcitrance, suggesting that ECM-driven stabilization operates independently of chemical persistence. ECM fungi constrained microbial oxidative enzyme investment, notably suppressing polyphenol oxidase, thereby reshaping microbial carbon processing. Plant-derived CAZymes dominated SOC depolymerization, while SOC partitioning was independently regulated by a *Bradyrhizobium–Penicillium*-centered microbial guild and by the CAZy enzyme families GH104 (bacterial) and GH17 (fungal). MAOC accumulation was more closely associated with microbial necromass formation and microbial carbon pump efficiency than with lignin chemistry. Collectively, these findings demonstrate that ECM symbiosis mediates soil carbon fate under N enrichment by coordinating microbial community composition, enzymatic activity, and necromass pathways, redirecting carbon from rapid mineralization to biologically mediated stabilization. This study highlights ECM fungi as critical biotic controllers of SOC persistence in N-enriched plantation ecosystems.

Project funding: This work was funded by the National Natural Science Foundation of China (32071639), and the Key Projects of Guangzhou of Science and Technology Plan (202206010019).

The online version is available at https://link.springer.com/.

Corresponding editor: Lei Yu.

Supplementary Information The online version contains supplementary material available at https://doi.org/10.1007/s11676-026-02082-3.

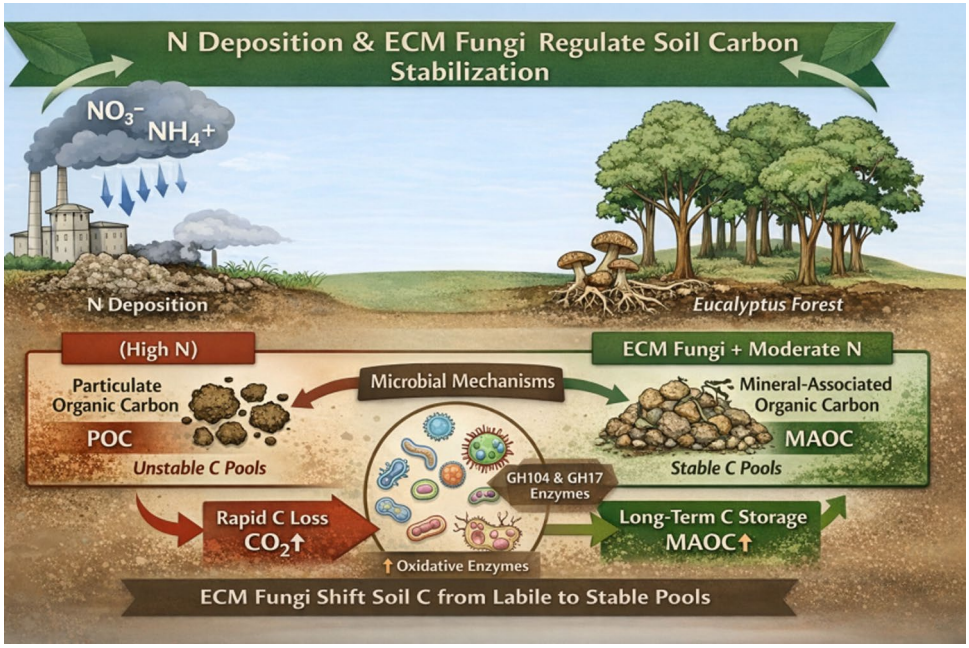
✉ Ming Tang
tangming@scau.edu.cn

[1] State Key Laboratory of Conservation and Utilization of Subtropical Agro-Bioresources, Guangdong Laboratory for Lingnan Modern Agriculture, College of Forestry and Landscape Architecture, South China Agricultural University, Guangzhou 510642, People's Republic of China

[2] Boone Pickens School of Geology, Oklahoma State University, Stillwater, OK 74074, USA

Published online: 05 June 2026

Graphical abstract



Keywords Ectomycorrhizal symbiosis · Nitrogen enrichment · Soil carbon pools · Microbial community · CAZymes · *Eucalyptus*

Introduction

Nitrogen (N) deposition, a major component of global environmental change, has profoundly altered biogeochemical cycles worldwide. As a critical limiting nutrient, reactive N can stimulate plant growth; however, chronic N enrichment frequently disrupts ecosystem functioning by altering biodiversity, soil chemistry, and nutrient cycling processes (Stevens et al. 2004; Galloway et al. 2008). China, historically a hotspot of atmospheric N deposition, has recently experienced a decrease in deposition rates, from 20.4 ± 2.6 kg ha^{-1} a^{-1} during 2011–2015 to 14.6 ± 3.0 kg ha^{-1} a^{-1} in 2015–2020 (Yu et al. 2019; Liu et al. 2024; Wu et al. 2025). Elevated N deposition exerts complex and sometimes contradictory effects on the terrestrial carbon cycle, particularly affecting the persistence and composition of soil organic carbon (SOC), the largest carbon pool in terrestrial ecosystems, and even minor changes in its stability can markedly influence climate feedbacks (Reay et al. 2008; Zhang et al. 2026). In forest ecosystems, N deposition regulates SOC stability through multiple, often contrasting mechanisms. On the one hand, N enrichment can suppress microbial decomposition and oxidative enzyme activities, thereby reducing litter decay rates and promoting SOC accumulation (Frey et al. 2014). On the other hand, N addition may alter plant carbon allocation patterns, microbial community composition, and extracellular enzyme production, which in turn affects the formation and persistence of SOC fractions, such as particulate organic carbon (POC) and mineral-associated organic carbon (MAOC) (Lu et al. 2021). Emerging evidence further suggests that N-induced shifts in microbial carbon use efficiency and residue production regulate the contribution of microbial necromass to stable SOC pools (Liang et al. 2017). Moreover, N-driven changes in soil acidity and organic–mineral interactions may regulate the stabilization and destabilization of MAOC in forest soils (Willard et al. 2026). Despite these advances, it remains unclear to what extent N enrichment alters the relative contributions of plant-derived versus microbially processed carbon to SOC stabilization, particularly across spatially distinct compartments associated with ectomycorrhizal (ECM) fungi, such as the mycorrhizosphere and hyphosphere.

The persistence of SOC is increasingly understood to be governed not only by the quantity of plant-derived inputs but also by microbial transformation processes that regulate carbon stabilization. Contemporary frameworks emphasize that microbial carbon use efficiency, residue formation, and subsequent interactions with soil minerals are central to long-term SOC sequestration. In this context, microbial necromass has been recognized as a dominant precursor of stable SOC, a process conceptualized as the microbial carbon pump (MCP) (Liang et al. 2017). In parallel, a fraction of

plant-derived compounds, particularly structurally complex polymers such as lignin, may also contribute directly to SOC persistence depending on their degree of microbial processing and physicochemical protection (Cotrufo et al. 2015). Consequently, SOC stability reflects the relative contributions and interactions between microbe-derived and plant-derived pathways across distinct SOC pools, including POC and MAOC (Lehmann et al. 2020).

N enrichment can decouple these SOC formation pathways by selectively altering microbial community composition and function. Elevated N availability often suppresses oxidative enzyme activities involved in the depolymerization of complex organic matter, potentially reducing SOC mineralization rates. Simultaneously, N addition frequently shifts microbial communities toward fast-growing, resource-acquisitive bacteria at the expense of slower-growing fungi, thereby reshaping microbial residue production and turnover (Fang et al. 2018; Tian et al. 2019; Ullah et al. 2021). Despite these general trends, reported effects of N enrichment on microbial necromass accumulation and SOC stabilization remain highly variable across ecosystems (Liang and Balser 2012; Hu et al. 2022). This variability suggests that key biological regulators mediating microbial responses to N enrichment are not yet fully incorporated into current conceptual models.

ECM fungi represent a potentially critical yet underexplored regulator within this framework. Forming symbiotic associations with many dominant forest tree species, ECM fungi occupy a strategic position at the interface of plant and soil C–N cycles (Wang et al. 2025). They receive substantial plant-derived carbon (primarily sugars and fatty acids) in exchange for facilitating N acquisition, often through the decomposition of organic matter (Smith and Read 2008; Lindahl and Tunlid 2015). This functional niche endows ECM fungi with a dual capacity in SOC dynamics: they can influence the fate of plant-derived carbon inputs while simultaneously contributing directly to persistent SOC through the production and accumulation of fungal necromass (Clemmensen et al. 2013). Importantly, N deposition is expected to perturb this balance by reducing the reliance of ECM fungi on organic N acquisition, suppressing extracellular enzyme production, and altering fungal biomass and turnover (Bödeker et al. 2014; Mielke et al. 2025). However, mechanistic understanding of how N availability regulates the relative contributions of ECM-derived necromass versus plant-derived residues to distinct SOC pools remains limited.

An additional but largely overlooked dimension is the spatial heterogeneity of ECM-mediated SOC processes. Carbon transformation and stabilization may differ markedly between the mycorrhizosphere, where roots, fungi, and bacteria interact intensely, and the extraradical hyphosphere, dominated by fungal hyphae with limited root influence. N deposition may further amplify this spatial differentiation by altering carbon allocation patterns, microbial competition, and enzyme expression across these niches. Yet empirical studies explicitly disentangling niche-specific SOC formation pathways under ECM symbiosis are scarce.

Eucalyptus spp., widely planted across subtropical China, provide an ideal model system for addressing these knowledge gaps due to their capacity to form associations with both ectomycorrhizal and arbuscular mycorrhizal fungi (Visscher et al. 2020). Growing concerns over soil sustainability in intensively managed Eucalyptus plantations further underscore the need to elucidate mechanisms governing SOC persistence. Recent evidence suggests that both ECM symbiosis and N addition alter belowground carbon allocation in *Eucalyptus* systems (He et al. 2024), implying downstream consequences for SOC composition and stability.

Here, we pose the following questions: (1) How do ECM fungi regulate the composition and stability of distinct SOC pools under increasing N availability? (2) To what extent does spatial differentiation between the mycorrhizosphere and hyphosphere underpin ECM-mediated SOC stabilization under N enrichment? (3) How do microbial diversity, keystone taxa, and functional potential interact with N availability and carbon sources to govern SOC persistence under ECM symbiosis?

Based on these questions, we hypothesize that N deposition alters microbial community composition and functional attributes, thereby influencing SOC stabilization processes in a spatially structured manner across the mycorrhizosphere and hyphosphere. Specifically, ECM fungi affect SOC persistence by regulating plant-derived carbon input and contributing fungal-derived residues to stable SOC pools, with the relative importance of these pathways varying spatially under N enrichment.

To test this hypothesis, we conducted a controlled experiment integrating biomarker analyses (amino sugars and lignin phenols), solid-state ^{13}C NMR spectroscopy, and metagenomic sequencing. We examined the effects of a gradient of N addition (0, 5, 10, and 20 mM) and inoculation with two ECM fungi (*Laccaria laccata* and *Tricholoma matsutake*) on SOC pool composition, microbial community structure, and functional potential in the mycorrhizosphere and hyphosphere of *Eucalyptus grandis* × *Eucalyptus urophylla*.

Materials and methods

Plant material, substrate, and ECM fungi inoculum preparation

E. grandis × *E. urophylla* seedlings were provided by the Research Institute of Tropical Forestry, Chinese Academy of Forestry. Seedlings approximately 15 cm in height were acclimatized in a greenhouse for one week prior to the experiment. To minimize interference from indigenous fungi, seedlings were immersed in a 0.5 g L^{-1} benomyl solution at 25 °C for 24 h. Following fungicide treatment, roots were carefully pruned to a uniform length of ~ 10 cm to standardize initial root biomass and architecture across all individuals.

Seedlings were grown in plastic pots (23 cm × 21 cm) containing 8 kg of autoclave-sterilized soil collected from the SCAU arboretum, passed through a 2 mm sieve, and sterilized by autoclaving (121 °C, 101 kPa, 2 h). Post-sterilization, soils were stored in a covered, ventilated room for 24 h prior to use to prevent recontamination. The soil, classified as Red soil under the Chinese system (equivalent to Ferralic Acrisols in FAO classification; Staff 2014), had a pH of 4.31 (1:2.5 soil:water), organic carbon content of 9.89 g kg^{-1}, available nitrogen of 0.03 mg g^{-1}, and available phosphorus of 80.15 mg kg^{-1}, measured following standard protocols (Plett et al. 2024).

Two ECM fungal strains, *Laccaria laccata* and *Tricholoma matsutake*, were isolated from the roots of *E. grandis* in the SCAU arboretum. Fungal strains were activated on modified Melin-Norkrans (MMN) medium (composition provided in Supplementary Table S1) at 25 °C in darkness for 14 days. Actively growing mycelial plugs (5 mm in diameter) were aseptically excised from the edge of the colonies and transferred onto fresh MMN plates, which were incubated under the same conditions. After sufficient mycelial growth, the fungi were propagated in large-scale liquid MMN culture to produce inoculum for experimental use. Subcultures were regularly performed every 4–6 weeks to maintain vigorous growth. Fully developed mycelium from these cultures was harvested and used as the ECM inoculum for subsequent experiments. For ECM inoculation, five holes (1 cm diameter × 5 cm depth) were made around each seedling's root system. Each hole was filled with 10 g of inoculum (5 g *L. laccata* + 5 g T. *matsutake*) and then backfilled with sterilized soil. Non-inoculated seedlings served as controls. Seedlings were allowed to establish for one week prior to the start of measurements, during which no mortality or visible stress symptoms were observed.

Experimental design

The experiment followed a fully factorial design with two primary factors, resulting in a total of eight treatments: ECM inoculation (with or without) and N addition at four levels (0, 5, 10, and 20 mM urea, corresponding to 0, 20, 40, and 80 kg ha^{-1} a^{-1}, respectively). Each treatment included four biological replicates, with three pots per replicate serving as technical repeats. In ECM-inoculated treatments, two types of soil cores were established to differentiate the contributions of the mycorrhizosphere (M) and hyphosphere (H). Mycorrhizosphere cores were constructed using PVC tubes (7 cm diameter × 15 cm height) wrapped with 2 mm nylon mesh, allowing both root and hyphal penetration, while hyphosphere cores used PVC tubes wrapped with 40 µm nylon mesh, permitting hyphal entry but excluding roots. All cores were laterally perforated and filled with sterilized soil sieved through a 2-mm mesh. The remaining pot substrate consisted of a 1:1 (v/v) mixture of river sand and sterilized soil to standardize growth conditions across treatments.

N addition commenced four months after ECM inoculation, allowing sufficient time for stable mycorrhizal colonization. From September 2022 to December 2023, 500 ml of urea solution was applied biweekly to each pot at concentrations corresponding to the designated N addition levels. This dosing scheme represented approximately 4–6 years of equivalent field-level N deposition when scaled to soil surface area (He et al. 2021; Geng and Jin 2022; Wu et al. 2023a, b). Environmental conditions were controlled in a greenhouse: relative humidity was maintained at 55%, daytime and nighttime temperatures were set to 26 °C and 20 °C, respectively, and a 16 h light/8 h dark photoperiod was applied. To minimize microenvironmental variation, pots were randomly repositioned on a weekly basis. Light intensity under greenhouse lamps was approximately 150 µmol m^{-2} s^{-1} light irradiance, ensuring consistent photosynthetic conditions across all treatments.

Sampling

After completion of N addition treatments, surface litter was carefully removed. Soil cores (0–15 cm depth) were obtained with a cylindrical sampler (5 cm in diameter). For each treatment, soils from every three pots were pooled to generate a single composite sample, yielding a total of four composite samples per treatment. Following collection, the soils were sealed in airtight bags, kept under chilled conditions, and delivered to the laboratory within 2 h. After passing through a sterile 2-mm sieve to eliminate

coarse materials, each composite soil was divided into three portions: (1) air-dried for physicochemical measurements, (2) stored at 4 °C for enzyme activity and microbial biomass measurements (analyzed within 48 h), and (3) frozen at − 80 °C for metagenomic sequencing. Concurrently, fine roots were collected from the same pots, fixed in FAA solution, and used for assessment of ECM colonization.

ECM fungi colonization

For each root sample, 100–150 root tips were randomly selected. These tips were cleared in 5% KOH at 90 °C for 30 min prior to microscopic examination. They were then acidified in 2% HCl for 5 min, followed by staining with 0.12% tetrazolium blue at 90℃ for 20 min. After staining, the root tips were destained in a 1:1 (v/v) glycerol acid solution. The samples were then observed under a stereomicroscope (Leica S9i, Leica Microsystems, Wetzlar, Germany) to identify ECM colonization, which was characterized by their distinct blue-stained, swollen root tip morphology. ECM colonization was calculated using the following formula:

$$\mathrm{ECM}(\%) = \frac{\text{Number of colonized root tips}}{\text{Total number of obversed root tip quantity}} \times 100\% \quad (1)$$

Paraffin sections

Plant fine roots were collected, labeled, and trimmed to 2–3 mm segments. Samples underwent standard histological processing: sequential dehydration through an ethanol series, clearing in xylene, paraffin wax infiltration and embedding. Using a rotary microtome (Leica RM2245), 5-µm serial sections were cut, slide-mounted, and air-dried. Sections were stained using Safranin O and Fast Green for histological differentiation. Stained sections were examined and imaged under a light microscope for subsequent analysis. The detailed procedure is provided in Materials and Methods Section 2.5 of the Supplementary Materials.

Measurement of ECM fungal biomass

Fungal ergosterol was quantified by UPLC (ACQUITY UPLC M-Class, Waters). Specifically for ECM fungi, which rely on plant-derived carbon and cannot persist under carbon limitation, ECM-derived ergosterol was calculated as the difference in total soil ergosterol before and after a five-month cultivation period (Bååth et al. 2004; Hendricks et al. 2016). Soil samples (10 g) underwent ergosterol extraction using methanol and KOH saponification, followed by cyclohexane partitioning. Extracts were concentrated, reconstituted in methanol, filtered, and analyzed by UPLC with a C18 reverse-phase column, methanol mobile phase (95:5, v/v), flow rate of 1 ml min^{-1}, and detection at 282 nm. Ergosterol concentration was determined against a standard calibration curve (0.0005–0.02 mg ml^{-1}). The detailed procedure is provided in Materials and Methods Section 2.6 of the Supplementary Materials. Fungal biomass was calculated based on the measured ergosterol concentration, extraction volume, and recovery rate (determined using autoclaved soil spiked with ergosterol standard).

$$\text{Fungal biomass}(\mu g\, g^{-1}) = C \times V \times R \times 1000 \times \text{Moisture coefficient} \quad (2)$$

Quantification of soil carbon fractions

SOC was assessed using heated dichromate oxidation, and NH_4^+-N and NO_3^--N were extracted with 2 mol L^{-1} $CaSO_4{\cdot}2H_2O$ and KCl, respectively. After filtration through 0.22 µm membranes, nutrient concentrations were quantified using a flow analyzer (SmartChem®200, Westco, Italy). Microbial biomass carbon (MBC) was determined by chloroform fumigation–extraction after 24 h exposure to ethanol-free chloroform and extraction with 0.5 M K_2SO_4. Filtered extracts were analyzed on a TOC analyzer (Elementar, Hanau, Germany), and MBC was calculated from fumigated–non-fumigated differences. Dissolved organic carbon (DOC) was obtained by water extraction (10 g fresh soil, 50 ml deionized water, 30 min shaking), followed by centrifugation (10,000 rpm, 10 min), filtration (0.45 µm), and TOC analysis (TOC-VCPH, Shimadzu, Japan).

POC and MAOC were separated by particle-size fractionation with wet sieving (Yu et al. 2025). Soil (10 g) was dispersed in 50 ml sodium hexametaphosphate (5 g L^{-1}) by shaking for 18 h, followed by wet sieving at 53 µm. Material retained on the sieve (> 53 µm) was defined as POC, whereas the < 53 µm fraction in the filtrate was considered MAOC. Both fractions were rinsed to clarity, dried at 60 °C to constant mass, and their SOC contents were determined on a soil-mass basis. The detailed procedure is provided in Materials and Methods Section 2.7 of the Supplementary Materials.

Soil enzyme analysis

Four soil carbon-cycle enzyme activities were assayed with commercial kits (Solarbio, Beijing, China). These include two soil enzymes, cellobiohydrolase (S-CBH, EC 3.2.1.91) and β-1,4-glucosidase (S-β-GC, EC 3.2.1.21). They catalyze the breakdown of cellulose, hemicellulose,

and related polysaccharides into smaller sugars for microbial utilization (Chen et al. 2020). Additionally, two soil oxidative enzymes-polyphenol oxidase (S-PPO, EC 1.14.18.1) and lignin peroxidase (S-Lip, EC 1.11.1.14) were measured. They oxidize lignin, phenols, and other aromatic compounds, facilitating degradation of recalcitrant molecules (Sinsabaugh 2010). The detailed procedure is provided in Materials and Methods Section 2.8 of the Supplementary Materials.

The stability of the carbon pool was assessed using the carbon quality index (CQI), calculated as follows (Xu et al. 2025):

$$\mathrm{CQI} = \frac{\mathrm{lnPPO}}{\mathrm{lnPPO} + \mathrm{lnGC}} \tag{3}$$

Microbial necromass carbon

Soil samples underwent acid hydrolysis (6 M HCl, 105 °C, 8 h). Myo-inositol was added as an internal standard after cooling. Hydrolysates were sequentially filtered, evaporated, pH-adjusted (6.6–6.8), centrifuged, and freeze-dried; residues were redissolved in methanol, centrifuged, nitrogen-purged, and freeze-dried again to isolate amino sugars. Amino sugars were derivatized (hydroxylamine hydrochloride + 4-(dimethylamino)pyridine, 75–80 °C) to form aldononitrile acetates and analyzed by GC (Agilent 6890A, HP-5 column 30 m × 0.25 mm × 0.25 μm, FID). The detailed procedure is provided in Materials and Methods Section 2.9 of the Supplementary Materials.

Fungal necromass carbon (FNC) and bacterial necromass carbon (BNC) were calculated using established formulas (Liang et al. 2019; Yang et al. 2024):

$$\mathrm{FNC}\left(\mathrm{g\ kg^{-1}}\right) = \left(\frac{\mathrm{GluN}}{179.15} - \frac{2\mathrm{MurA}}{251.23}\right) \times 179.17 \times 9 \tag{4}$$

$$\mathrm{BNC}\left(\mathrm{g\ kg^{-1}}\right) = \mathrm{MurA} \times 45 \tag{5}$$

Microbial necromass carbon (MNC) was calculated as the sum of FNC and BNC. The MNC/SOC ratio represented MCP efficiency (Zhu et al. 2020), while the necromass accumulation coefficient (NAC) was calculated as MNC/MBC (Zhang et al. 2021).

Plant-derived necromass carbon pool

Lignin phenol extraction and quantification followed Ma et al. (2018) with minor modifications. Lignin phenols were measured via alkaline CuO oxidation (170 ℃, 2.5 h, O_2-free), followed by ethyl acetate separation, BSTFA derivatization, and GC analysis (Shimadzu GC-2010 PRO, HP-5 column). Phenols were classified as: Cinnamyl (p-coumaric acid, ferulic acid), Syringyl (syringaldehyde, syringic acid, syringone), Vanillyl (vanillin, vanillic acid, acetovanillone), and P-hydroxyl (p-hydroxybenzaldehyde, *p*-hydroxyacetophenone, p-hydroxybenzoic acid). Ratios of S/V, C/V, and P/(V + S) were calculated to assess lignin decomposition states. Lignin degradation was evaluated using Ad/Al ratios of V and S phenols, which rise with oxidative SOC decomposition. The detailed procedure is provided in Materials and Methods Section 2.10 of the Supplementary Materials.

SOC chemical composition

SOC chemical composition was characterized using solid-state ^{13}C CPMAS-NMR spectroscopy (Bruker AVANCE III HD 400 MHz). Samples underwent hydrofluoric acid (HF) pretreatment to remove paramagnetic minerals prior to analysis. Spectra were acquired at 10 kHz MAS frequency with ^{13}C resonance at 100.625 MHz using a 4 mm H/X dual-resonance probe (Yuan et al. 2020). The detailed procedure is provided in Materials and Methods Section 2.11 of the Supplementary Materials.

Spectral integration of the solid-state ^{13}C CPMAS-NMR spectra was performed using MestReNova software (v.14.0). Functional groups were categorized into four regions based on chemical shifts: alkyl-C: 0–45 ppm, O-alkyl C: 45–110 ppm, aromatic C: 110–160 ppm, carbonyl C: 160–210 ppm. To assess the chemical stability of SOC, the hydrophobicity index (HI) was calculated as:

$$\mathrm{HI} = \frac{\mathrm{AlkylC} + \mathrm{AromaticC}}{\mathrm{O\text{-}AlkylC} + \mathrm{CarbonlyC}} \tag{6}$$

Ratios of Aromatic C/O-Alkyl C and (Alkyl-C+Aromatic C)/O-Alkyl C were used to evaluate SOC decomposition (Bera et al. 2019).

DNA extraction, sequencing, and bioinformatics analysis

Genomic DNA (1 μg) was fragmented and used for library construction following standard procedures, including end repair, adapter ligation, purification, and PCR amplification. Libraries meeting quality thresholds were pooled and sequenced on the Illumina PE150 platform (Li et al. 2014; Qin et al. 2010).

Raw reads were quality-filtered to remove adapters, low-quality sequences, and ambiguous bases, and host

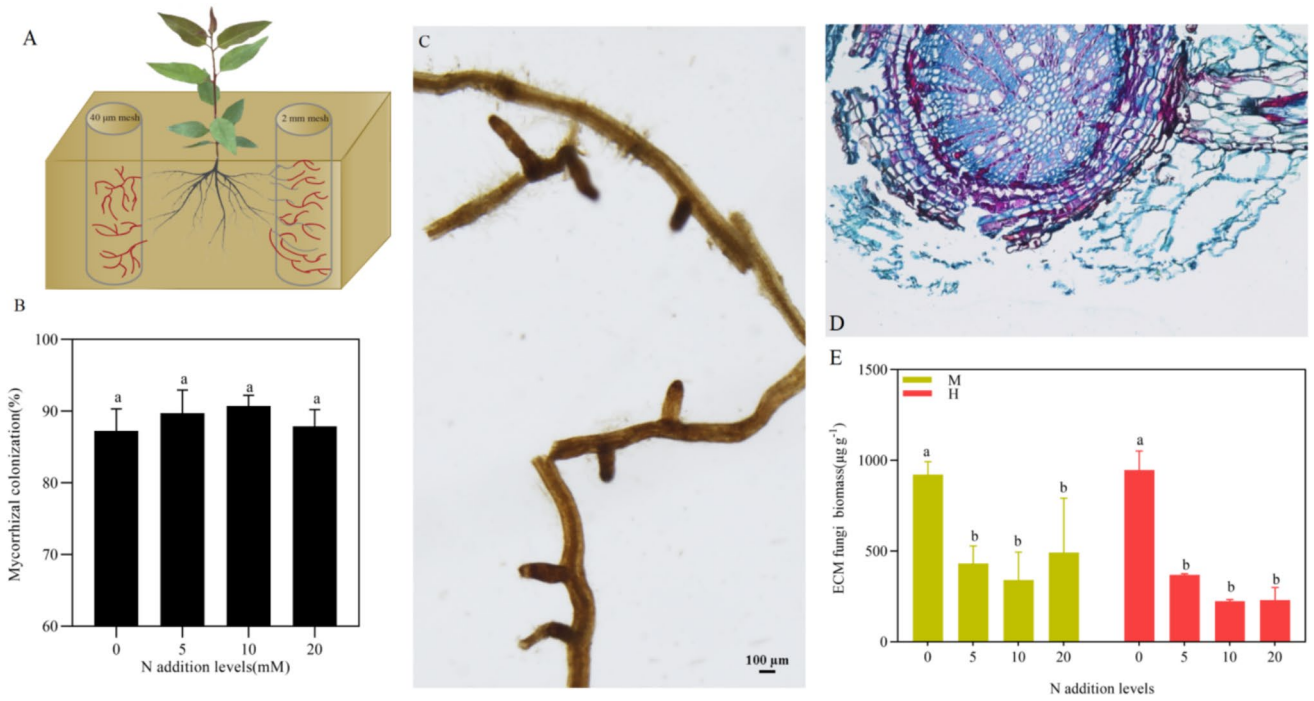


Fig. 1 Effects of N addition on ECM fungal colonization rate and biomass. **A** Schematic diagram of the mycorrhizal compartment; **B** ECM fungal colonization rate; **C** Mantle structure; **D** Hartig net; **E** ECM fungal biomass; M = mycorrhizosphere; H = hyphosphere

contamination was excluded (Karlsson et al. 2013). Clean reads were assembled, and open reading frames (ORFs) were predicted to construct a non-redundant gene catalog (Li et al. 2014; Sunagawa et al. 2015). Gene abundance was calculated based on read mapping results (Cotillard et al. 2013; Qin et al. 2014).

Taxonomic annotation was performed against a comprehensive microbial protein database using DIAMOND with LCA-based assignment (Huson et al. 2011; Buchfink et al. 2015). Functional annotation focused on carbohydrate-active enzymes using the CAZy database (Cantarel et al. 2009; Feng et al. 2015). Detailed parameters, software versions, and additional references are provided in Materials and Methods Section 2.12–2.13 of the Supplementary Materials.

Statistical analysis

All statistical analyses were conducted in R (v4.1.3) and SPSS (IBM Corp., Armonk, NY, USA). Data visualization, including bar plots and stacked bar plots, was generated using GraphPad Prism 8 (GraphPad Software, San Diego, CA, USA) and ggplot2 (v3.3.5). Two-way ANOVA was applied to assess treatment effects on soil carbon pools, enzyme activities, and microbial indices. Microbial community structure was analyzed by PCoA (ade4), with microbial community–carbon relationships evaluated using Mantel tests and RDA (vegan). Correlation heatmaps were produced using the corrplot package (v0.92). To identify key microbial taxa and enzyme families influencing soil carbon dynamics, a random forest model was constructed using the randomForest and pROC packages, with feature importance assessed for predictive interpretation.

Results

Effects of N addition on colonization rate and biomass of ECM fungi

Four months after inoculation, the ECM fungal colonization rate in *E. grandis* × *E. urophylla* root systems were assessed. Results revealed that ECM fungal colonization rates exceeded 80% across all N addition treatments, with no significant differences observed among treatments (Fig. 1B). In inoculated treatments, distinct mantle structures were clearly visible in the fine roots of giant eucalyptus (Fig. 1C). Following paraffin sectioning and Safranin-Fast Green staining, a well-defined Hartig net was observed, confirming successful colonization (Fig. 1D).

However, ECM fungal biomass progressively decreased with increasing N concentrations. Treatments with 5 to 20 mM N exhibited significantly reduced ECM fungal

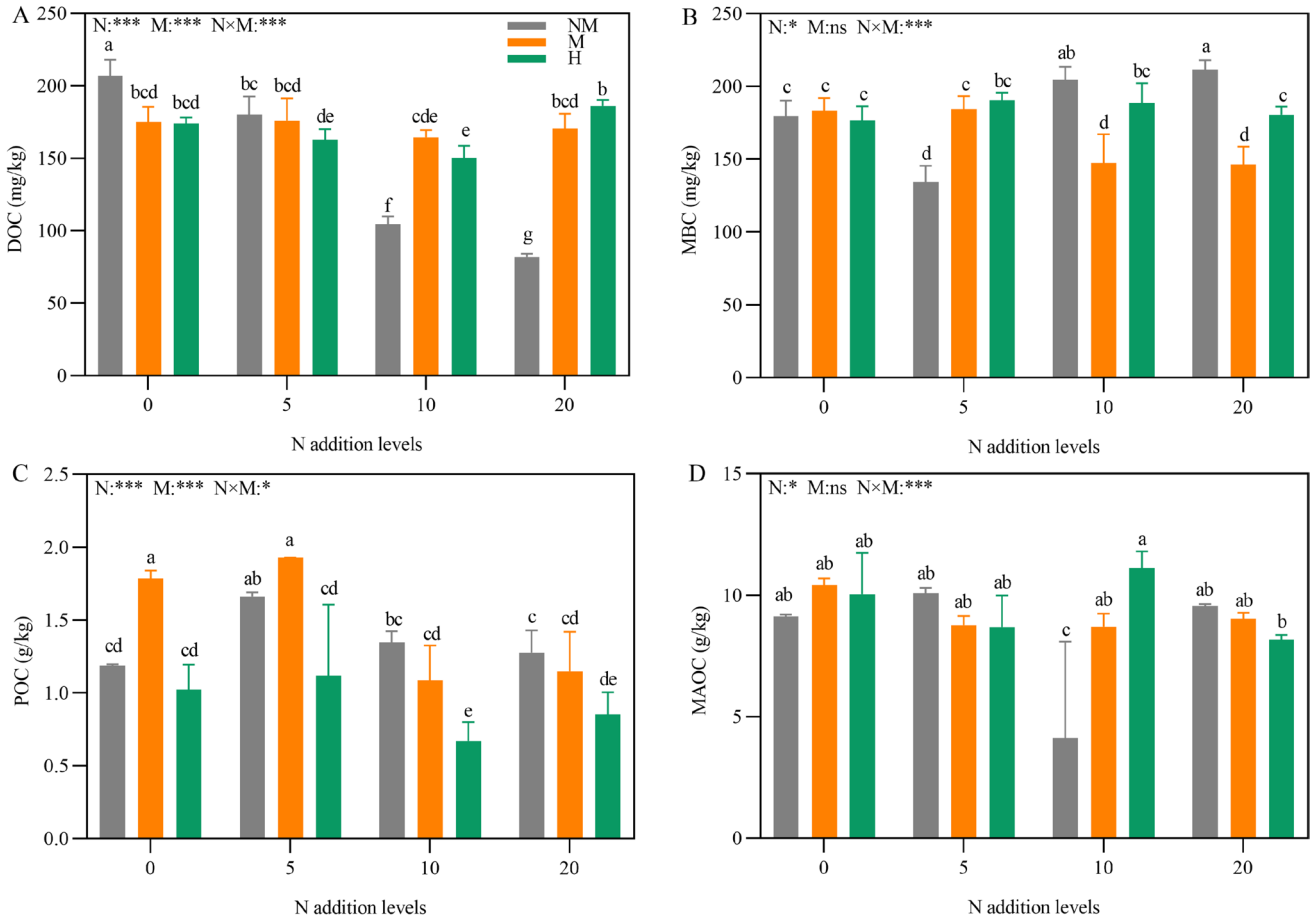


Fig. 2 Effects of ECM fungal inoculation and N addition on soil carbon pools. **A** DOC, **B** MBC, **C** POC, and **D** MAOC are presented across the N addition gradient in inoculated and non-inoculated soils. Data are means ± SE (n = 4). Different letters indicate significant differences ($p < 0.05$). N = N addition; NM = without inoculation; M = mycorrhizosphere; H = hyphosphere

biomass compared to the 0 mM N control ($p < 0.05$; Fig. 1E), indicating that elevated N addition suppressed ECM fungal growth in the soil.

N addition and ECM inoculation restructure soil carbon pools

N addition and ECM inoculation significantly altered the size and distribution of soil carbon pools (Fig. 2). Across the N addition gradient, DOC decreased progressively in non-inoculated soils, whereas ECM inoculation largely stabilized DOC concentrations, resulting in a significant N × ECM interaction (Fig. 2A). MBC responded primarily to the interaction between N addition and ECM inoculation: in non-inoculated soils, MBC increased with increasing N availability, whereas under ECM inoculation MBC declined significantly at 10–20 mM N addition, with MBC consistently higher in the hyphosphere than in the mycorrhizosphere at these N levels (Fig. 2B). POC exhibited a unimodal response to N addition, increasing at low N levels and peaking at 5 mM N, followed by a decline at higher N concentrations. ECM inoculation significantly increased POC at 5 mM N compared to non-inoculated soils but resulted in lower POC at 10–20 mM N, while POC concentrations in the hyphosphere were consistently lower than those in the mycorrhizosphere across all treatments (Fig. 2C). MAOC responded non-linearly to N addition, decreasing initially and reaching a minimum at 10 mM N, where ECM inoculation significantly increased MAOC relative to non-inoculated soils (Fig. 2D). Together with the low-N accumulation of POC, these patterns indicate contrasting responses of POC and MAOC to N addition and a shift in soil carbon pool partitioning (Fig. 2C–D).

N availability and ECM symbiosis regulate microbial carbon processing capacity

Activities of carbon-degrading enzymes responded distinctly to N addition and ECM inoculation (Fig. 3). Hydrolytic enzymes associated with labile carbon decomposition

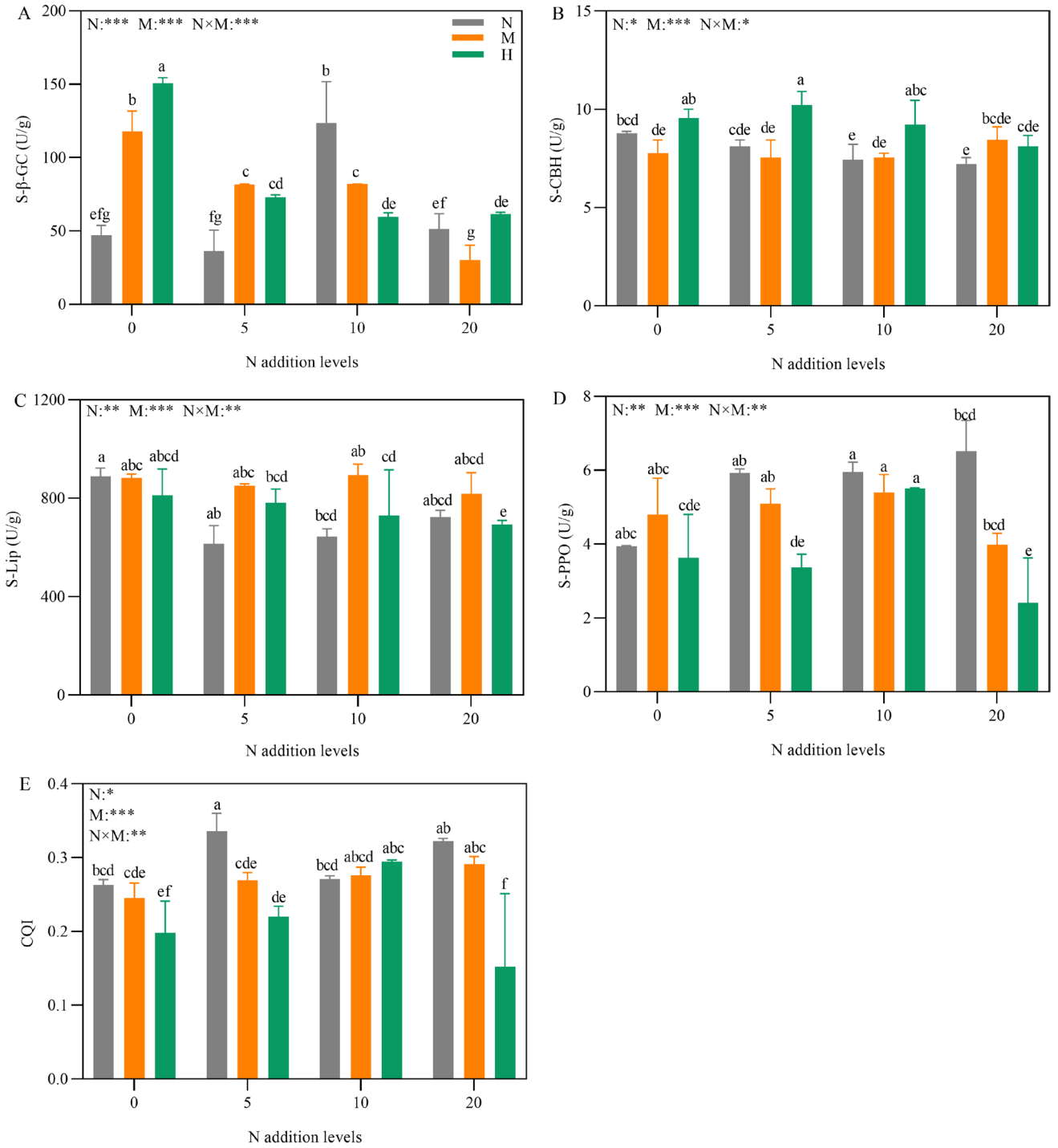


Fig. 3 Responses of soil carbon-degrading enzyme activities and carbon quality index to ECM fungal inoculation and N addition. **A** S-β-GC, **B** S-CBH, **C** S-Lip, and **D** S-PPO, as well as **E** CQI. Data are means ± SE (n = 4). Different letters indicate significant differences ($p < 0.05$). N = N addition; NM = without inoculation; M = mycorrhizosphere; H = hyphosphere

responded differently to N addition and ECM inoculation. In non-inoculated soils, S-β-GC activity exhibited a unimodal response, peaking at 10 mM N. Under ECM inoculation, S-β-GC activity declined progressively with increasing N addition, being significantly higher than in non-inoculated soils at 0–5 mM N but significantly lower at 10–20 mM N. In the hyphosphere, S-β-GC activity was significantly higher than in the mycorrhizosphere at 0 and 20 mM N (Fig. 3A). S-CBH activity was not significantly affected by ECM inoculation across N treatments but was consistently higher in

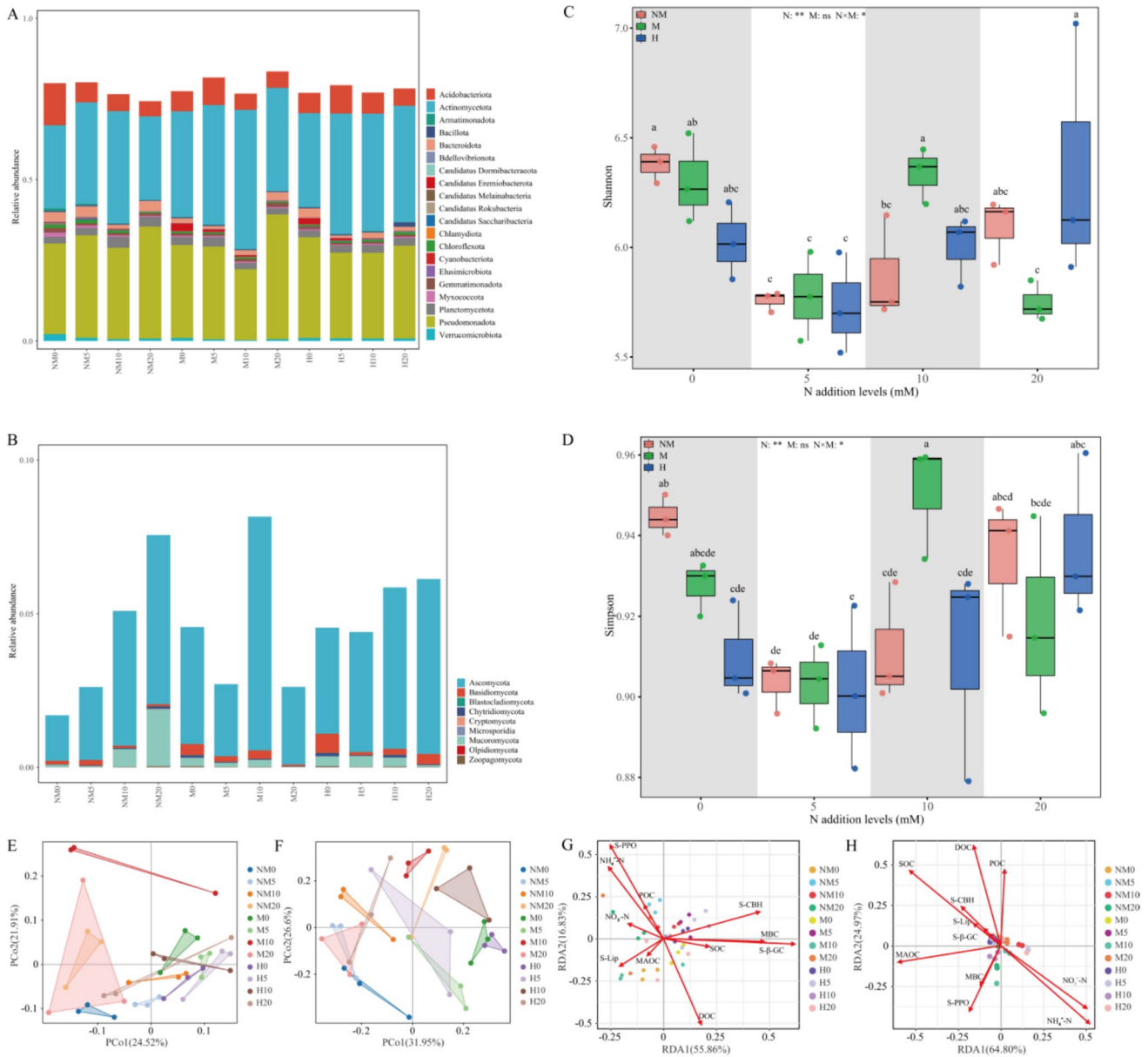


Fig. 4 Effects of ECM fungal inoculation and N addition on soil microbial community composition and diversity. **A**, **B** Relative abundances of dominant bacterial and fungal phyla. **C**, **D** Shannon and Simpson diversity indices. **E**, **F** PCoA showing β-diversity patterns for bacterial and fungal communities. **G**, **H** RDA showing the relationships between bacterial and fungal community compositions and soil environmental variables, respectively

the hyphosphere than in the mycorrhizosphere at 0–10 mM N (Fig. 3B). In contrast, oxidative enzymes displayed strong sensitivity to N addition and ECM inoculation: S-Lip activity declined with increasing N addition in non-inoculated soils but remained relatively stable under ECM inoculation, while S-PPO activity increased along the N gradient in non-inoculated soils but was significantly suppressed by ECM inoculation at 5–20 mM N, with lower hyphosphere activity than mycorrhizosphere at 5 and 20 mM N (Fig. 3C–D). The CQI varied significantly among treatments, exhibiting a unimodal response to N addition with a peak at 5 mM N, and was generally reduced under ECM inoculation, particularly in the hyphosphere (Fig. 3E).

ECM fungi and N addition reshape microbial community structure and diversity

Both N addition and ECM inoculation significantly influenced microbial community composition and diversity in *E. grandis* × *E. urophylla* soils (Fig. 4; Table S2).

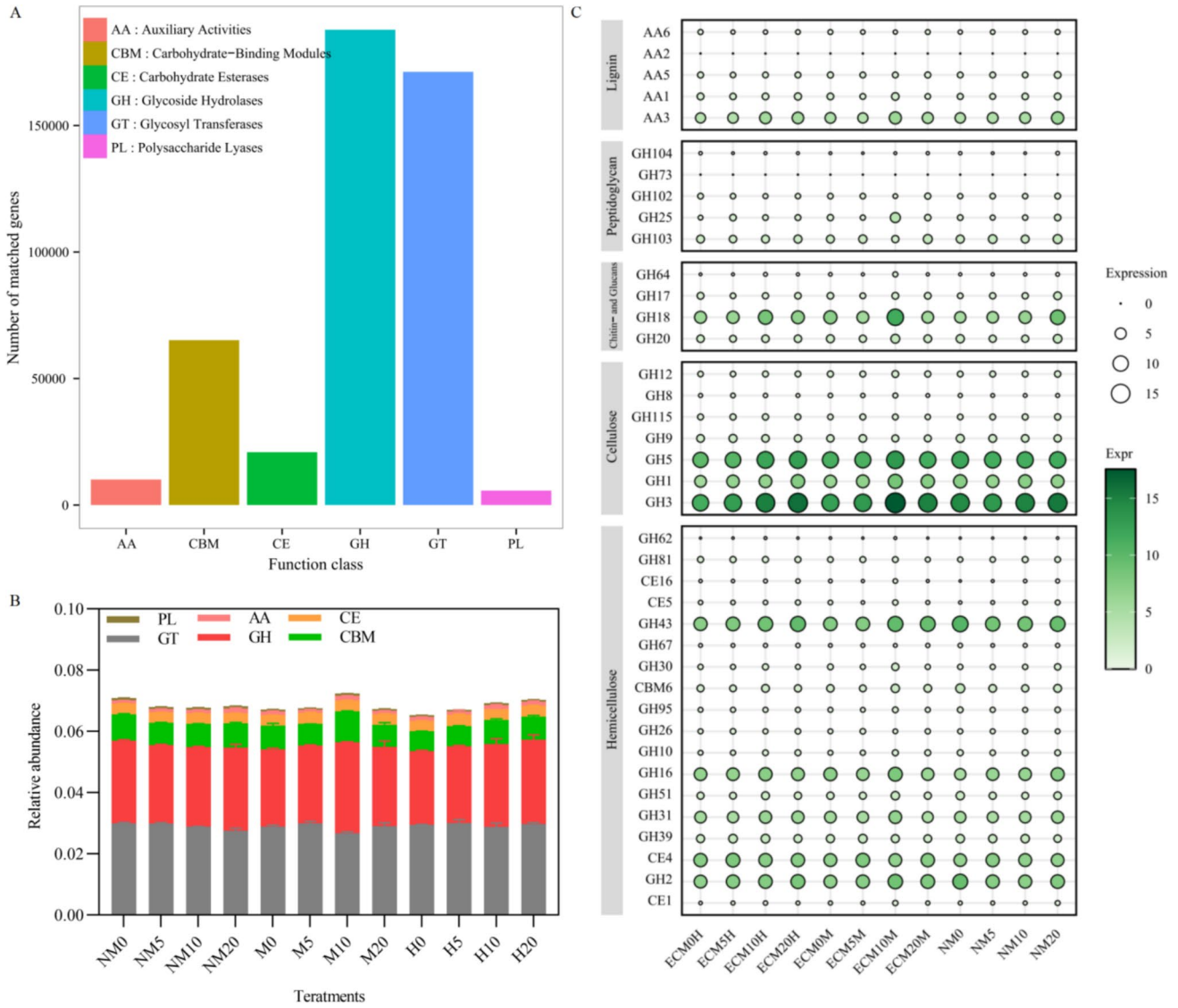


Fig. 5 Composition and distribution of carbohydrate-active enzyme (CAZy) genes under ECM fungal inoculation and N addition. **A** Relative abundance of major CAZy classes. **B** Stacked distribution of CAZy classes across treatments. **C** Heatmap showing variation in dominant CAZy families involved in carbon degradation. Color intensity indicates normalized gene abundance

Bacterial communities were dominated by Actinomycetota (33.51%), Pseudomonadota (29.52%), and Acidobacteriota (6.74%), whereas Ascomycota (> 4.03%) prevailed among fungi, with Mucoromycota peaking at 0.63% under high N with ECM inoculation (Fig. 4A–B). At the genus level, Conexibacter (11.87%) led bacterial decomposers, while Penicillium (1.29%) was the most abundant fungal genus and increased with N addition (Fig. S1C–D). Alpha diversity indices of bacterial and fungal communities showed U-shaped responses to increasing N availability, with minimum Shannon and Simpson values at 5 mM N, and ECM inoculation generally moderated these effects, particularly in the hyphosphere (Fig. 4C–D). PCoA revealed clear separation of bacterial and fungal communities along the N gradient and between ECM treatments (Fig. 4E–F). RDA identified significant environmental drivers of microbial community composition: bacterial communities were primarily structured by S-β-GC, DOC and S-PPO (cumulative variance 72.69%), whereas fungal communities responded to MAOC, NH_4^+-N, NO_3^--N, SOC and DOC (cumulative variance 89.77%; Fig. 4G–H).

Functional potential for carbon transformation revealed by metagenomic CAZy profiles

Metagenomic analysis revealed distinct shifts in the functional potential for soil carbon transformation across N addition and ECM inoculation treatments, as reflected by CAZy gene profiles (Fig. 5; Table S2–S6).

Genes associated with carbohydrate hydrolysis, including glycoside hydrolases (GHs) and carbohydrate esterases (CEs), were most abundant under all treatments, with GHs showing the highest gene counts (187,857) followed by glycosyl transferases (GT, 171,197) and carbohydrate-binding modules (CBM, 65,139), whereas auxiliary activity enzymes (AAs) exhibited lower relative abundance and contrasting responses across N × ECM conditions (Fig. 5A–B). Plant-derived enzymes dominated (> 80% of total abundance), targeting hemicellulose, cellulose, and lignin, while bacterial and fungal contributions were minor, including peptidoglycanases and chitinases/glucanases, respectively (Fig. 5C).

Microbial necromass and plant-derived residues drive contrasting SOC stabilization pathways

Biomarker analyses revealed divergent responses of microbe- and plant-derived SOC components to N addition and ECM inoculation (Fig. 6; Table S6). Amino sugar-derived MNC, particularly FNC, responded strongly to N × ECM interactions. Under ECM inoculation, FNC declined progressively with increasing N addition and was significantly lower than in non-inoculated soils at 5–10 mM N, whereas hyphosphere FNC was consistently higher than mycorrhizosphere FNC at 5–20 mM N (Fig. 6A). Similar response patterns were observed for total MNC and MCP efficiency, both of which were significantly regulated by N addition, ECM inoculation, and their interaction (Fig. S2A; Fig. 6B).

Lignin phenol composition was dominated by V-type monomers, whereas C-type monomers were least abundant across all treatments (Fig. S4; Table S8). Both N addition and ECM inoculation altered lignin monomer ratios, with pronounced effects on the C/V and S/V indices (Fig. 6C–D).

The C/V ratio exhibited clear spatial differentiation, with consistently higher values in the hyphosphere than in the mycorrhizosphere under 0–10 mM N (Fig. 6C). In contrast, ECM inoculation significantly increased the S/V ratio under high N availability, with ECM-inoculated soils showing higher S/V values than non-inoculated controls at 20 mM N ($p < 0.05$; Fig. 6D).

Solid-state ^{13}C NMR analysis revealed pronounced shifts in SOC chemical composition along the N addition gradient (Fig. S6; Table S9), as reflected by changes in the alkyl-to-aromatic C/O-alkyl C ratio and the hydrophobicity index (Fig. 6E–F). Both indices increased progressively with increasing N addition, indicating enhanced chemical recalcitrance of SOC under N enrichment. However, ECM inoculation consistently reduced the alkyl-aromatic C/O-alkyl C ratio and hydrophobicity index across all N treatments compared with non-inoculated soils.

Integrative analyses identify key drivers of SOC pool stabilization

Integrative statistical analyses identified key microbial taxa and functional enzymes as major drivers of soil carbon pool dynamics (Fig. 7). Random forest analysis revealed that a limited number of bacterial and fungal genera accounted for a large proportion of the variance in SOC pools. The top six bacterial genera involving *Bradyrhizobium*, *Geodermatophilus*, *Edaphobacter*, *Phenylobacterium*, *Candidatus Koribacter*, and *Actinospica* collectively explained 40.8% of the total variance (Fig. S5A). Similarly, six fungal genera (*Penicillium*, *Thelephora*, *Aspergillus*, *Trichoderma*, *Rhizopus*, and *Jimgerdemannia*) accounted for 39.68% of the explained variance in soil carbon pools (Fig. S5B).

Microbial attributes and CAZy functional groups exhibited distinct associations with soil carbon pools. CQI was strongly correlated with S-PPO activity, whereas MCP efficiency was positively linked to FNC and NAC. Bacterial necromass decreased with NH_4^+–N, while SOC hydrophobicity increased with inorganic N and decreased with DOC. Fungal relative abundance was positively associated with hydrolytic enzyme activities, BNC, and NO_3^-–N, showing stronger links to hydrophobicity and NH_4^+–N (Fig. 7A). Plant-derived CAZymes driving plant carbon depolymerization correlated with O-alkyl C, hydrophobicity, and the alkyl-to-aromatic C/O-alkyl C ratio, whereas microbial-derived CAZymes were positively linked to MBC (Fig. S6). RDA analysis demonstrated that CAZy enzyme families exerted significant influences on DOC, SOC, and MAOC pools (Fig. 7B). In contrast, linear regression analyses revealed source-specific negative relationships, with bacterial-derived CAZy enzyme families negatively correlated with MBC, fungal-derived enzyme families negatively correlated with DOC, and plant-derived enzyme families negatively correlated with SOC, respectively (Fig. 7C–E).

Random forest modeling identified enzyme-level drivers of individual SOC pools (Fig. 7F–H; Fig. S5C–D). MBC was driven by 6 families (31.50%), primarily plant-derived, with fungal GH17 as the principal microbial-associated predictor (Fig. 7F). DOC variation was mainly explained by 11 enzyme families (54.56% cumulative contribution), dominated by plant-derived CAZymes, with bacterial GH104 and fungal GH17 as notable contributors (Fig. 7G). POC and MAOC dynamics were regulated by six (29.46%) and four (23.73%) enzyme families, respectively, largely plant-derived CAZymes with consistent contributions from bacterial GH104 (Fig. 7H;

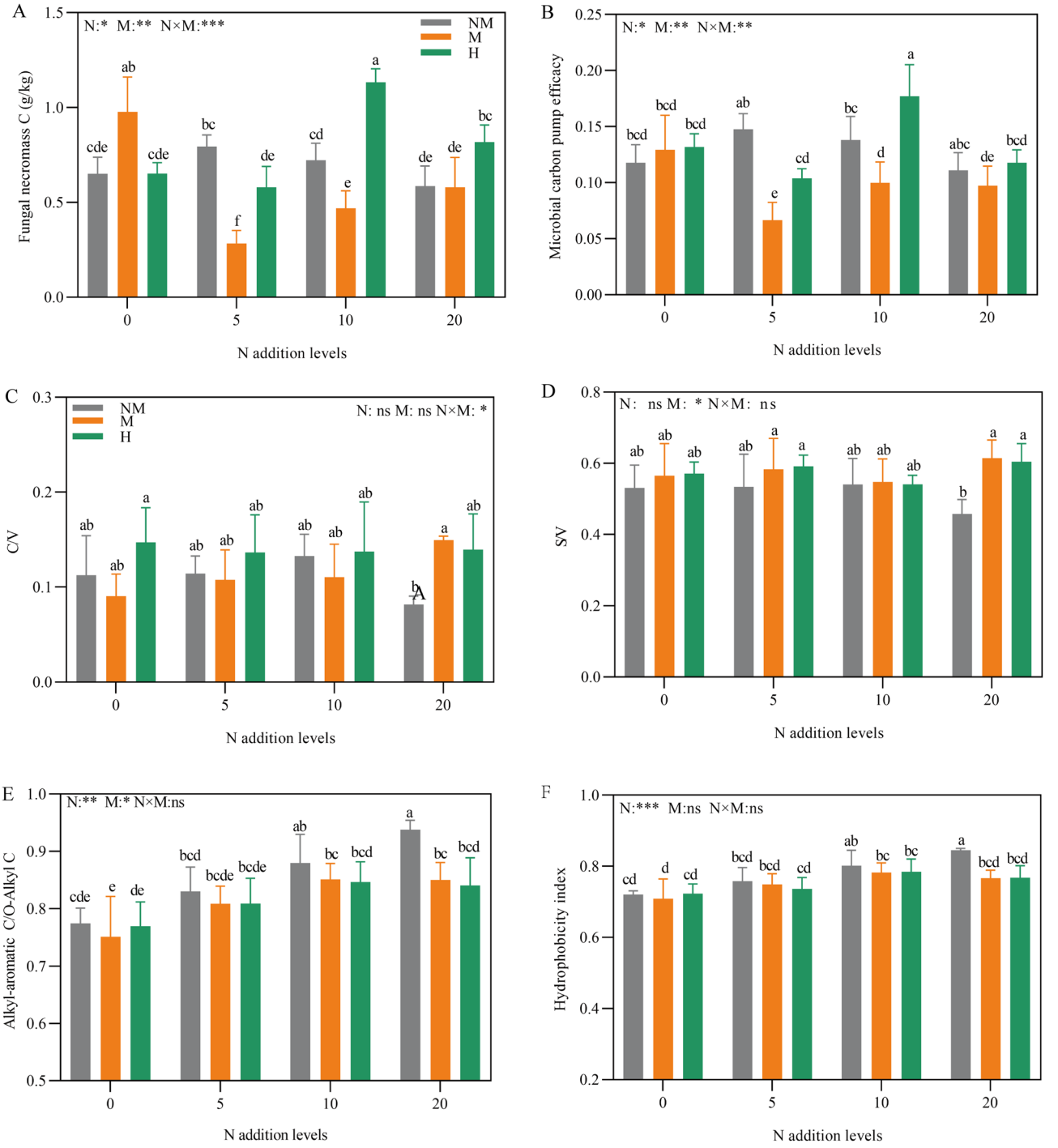
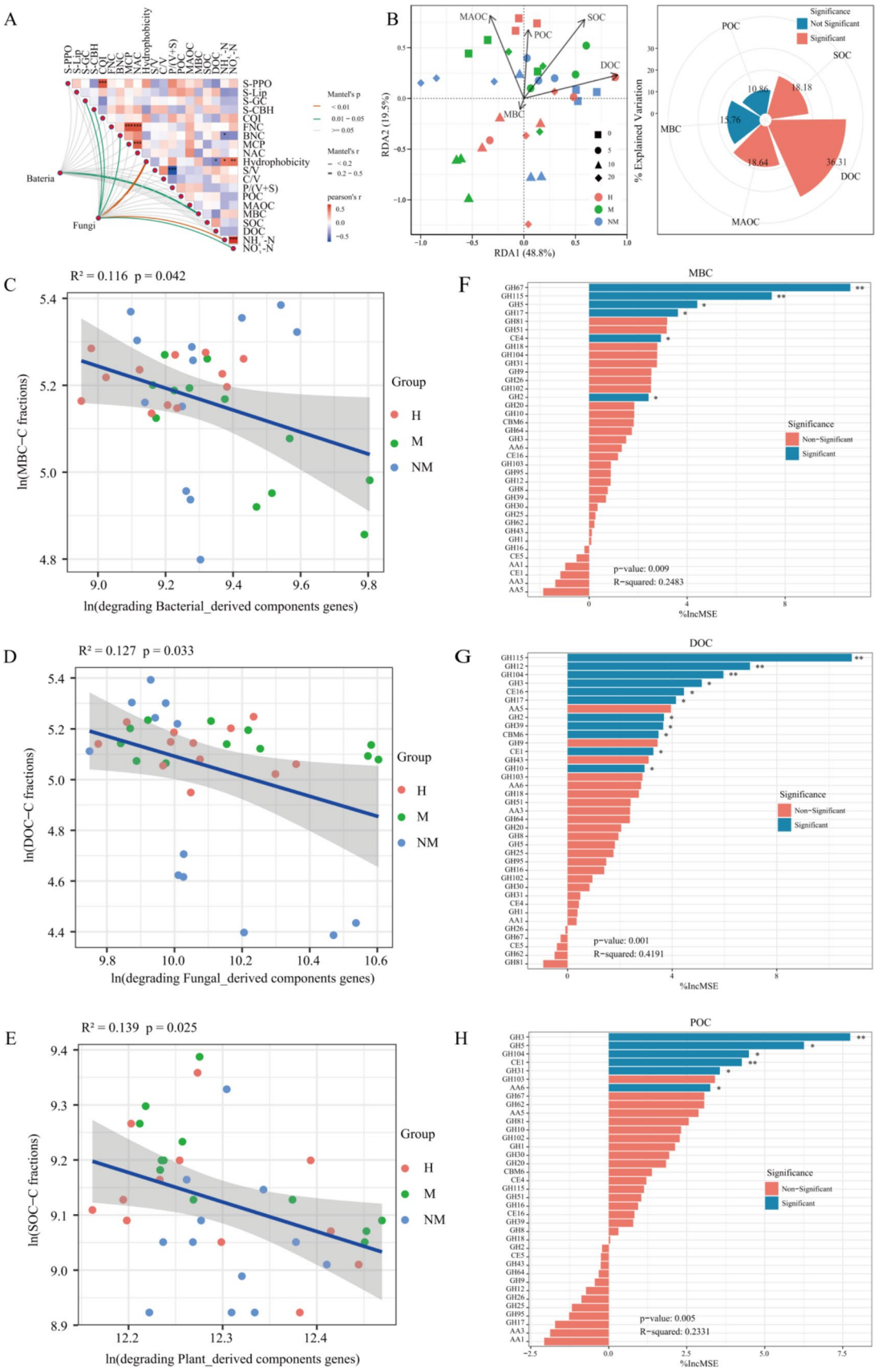


Fig. 6 Indicators of soil organic carbon chemical composition and origin under ECM inoculation and N addition. **A** Shown are fungal-derived amino sugars. **B** Microbial carbon pump efficiency. **C**, **D** Lignin phenol ratios (C/V and S/V). **E**, **F** ^{13}C-NMR–derived indices including the alkyl-aromatic C/O-alkyl C ratio and hydrophobicity index. Data are means ± SE (n = 4). Different letters indicate significant differences ($p < 0.05$). N = N addition; NM = without inoculation; M = mycorrhizosphere; H = hyphosphere

Fig. S5C). SOC variation was associated exclusively with plant-derived enzyme families (14.85% cumulative contribution; Fig. S5D).

Overall, plant-derived CAZymes dominated enzymatic regulation across SOC pools, whereas only GH104 (bacterial) and GH17 (fungal) consistently emerged as key microbial predictors, indicating functional redundancy among plant-associated


A
S-PPO
S-Lip
S-GC
S-CBH
CQI
FNC
BNC
MCP
NAC
Hydrophobicity
S/V
C/V
P/(V+S)
POC
MAOC
MBC
SOC
DOC
NH4+-N
NO3--N
Bateria
Fungi
Mantel's p
< 0.01
0.01 ~ 0.05
>= 0.05
Mantel's r
< 0.2
0.2 ~ 0.5
pearson's r
0.5
0.0
−0.5
B
MAOC
SOC
POC
DOC
MBC
RDA2 (19.5%)
RDA1 (48.8%)
0
5
10
20
H
M
NM
Significance
Not Significant
Significant
% Explained Variation
10.86
18.18
15.76
18.64
36.31
C
R² = 0.116 p = 0.042
ln(MBC−C fractions)
ln(degrading Bacterial_derived components genes)
Group
H
M
NM
F
MBC
Significance
Non−Significant
Significant
p−value: 0.009
R−squared: 0.2483
%IncMSE
D
R² = 0.127 p = 0.033
ln(DOC−C fractions)
ln(degrading Fungal_derived components genes)
G
DOC
p−value: 0.001
R−squared: 0.4191
E
R² = 0.139 p = 0.025
ln(SOC−C fractions)
ln(degrading Plant_derived components genes)
H
POC
p−value: 0.005
R−squared: 0.2331

◂**Fig. 7** Linkages between microbial-derived CAZy enzyme families and soil carbon pools. **A** Mantel test showing correlations between the relative abundances of bacterial and fungal communities and soil carbon pool parameters. **B** RDA illustrating relationships between CAZy enzyme families and different soil carbon pools. **C**–**E** Linear regression analyses depicting relationships between bacterial-derived CAZy enzyme families and microbial biomass carbon (MBC; **C**), fungal-derived CAZy enzyme families and dissolved organic carbon (DOC; **D**), and plant-derived CAZy enzyme families and soil organic carbon (SOC; **E**). **F**–**H** Random forest analysis identifying the relative importance of CAZy enzyme families in explaining variations in different soil carbon pools

enzymes and niche-specific roles of select microbial functions in SOC stabilization.

Discussion

ECM fungi shift SOC stabilization pathways under N enrichment

N enrichment reshaped SOC stabilization primarily by redistributing carbon between particulate and mineral-associated pools rather than by uniformly increasing total SOC. Along the N gradient, POC preferentially accumulated under low N availability but declined with increasing N inputs, whereas MAOC exhibited a delayed, non-linear response, reaching a minimum at intermediate N levels. Under low N conditions, enhanced plant-derived carbon inputs combined with constrained microbial decomposition efficiency likely favored the transient accumulation of relatively unprotected particulate organic matter (Wu et al. 2023a, b). As N availability increased, stimulated microbial activity and enzymatic investment accelerated the decomposition of labile particulate substrates, resulting in a net decline in POC pools (Liu et al. 2025).

ECM inoculation fundamentally altered SOC partitioning by selectively enhancing MAOC accumulation at 10 mM N addition. Notably, this increase occurred despite concurrent declines in SOC hydrophobicity and chemical recalcitrance, as indicated by reduced alkyl-aromatic C and O-alkyl C ratios and lower hydrophobicity indices derived from ^{13}C NMR spectra. This decoupling between chemical composition and carbon persistence suggests that ECM fungi promote the transfer of carbon from rapidly cycling particulate pools into mineral-associated forms through biologically mediated mechanisms, likely involving enhanced microbial necromass production and stronger mineral surface interactions, rather than through selective preservation of chemically resistant compounds (Guan et al. 2025).

Together, these results indicate that SOC persistence under N enrichment is not governed primarily by increasing chemical recalcitrance. Instead, ECM fungi enhance SOC stabilization by promoting mineral association even as SOC becomes chemically more labile, reflecting a shift from chemistry-driven to biologically mediated stabilization pathways (Chen et al. 2025a). Within this framework, changes in POC mainly reflect shifts in carbon input-decomposition balance along the N gradient, whereas ECM fungi regulate longer-term SOC persistence by redirecting particulate carbon into mineral-associated pools rather than stabilizing POC per se (Wang et al. 2021).

N-induced changes in microbial carbon processing and enzyme investment

The shift in SOC pool partitioning under N enrichment—particularly the ECM-induced increase in MAOC at intermediate N levels—cannot be explained by changes in SOC chemical recalcitrance alone (Hu et al. 2024). Instead, these patterns point to altered microbial carbon processing pathways, suggesting that ECM fungi regulate SOC stabilization primarily through controlling decomposition processes rather than through selective preservation of chemically inert carbon fractions (Guan et al. 2025). This highlights microbial enzyme investment strategies as a key mechanistic link between N inputs and SOC stabilization outcomes. N addition restructured microbial enzyme allocation in non-inoculated soils toward enhanced oxidative decomposition (Chen et al. 2025b). Along the N gradient, increased S-PPO activity reflects greater microbial investment in oxidative enzymes targeting chemically complex substrates, consistent with enzyme allocation theory predicting enzymatic reallocation following relaxation of nutrient constraints (Allison and Vitousek 2005). This response implies that alleviation of N limitation under elevated N availability enables microorganisms to access more recalcitrant carbon pools.

In contrast, ECM inoculation constrained this N-stimulated oxidative pathway. Strong suppression of S-PPO activity, particularly at moderate to high N levels, indicates that ECM fungi exert effective control over oxidative decomposition. This suppression extended, albeit more weakly, to hydrolytic enzymes such as β-glucosidase, reflecting a coordinated downregulation of microbial carbon-degrading capacity under ECM influence. These responses support the concept of ECM fungi as "gatekeepers of decomposition", limiting microbial access to both labile and structurally complex carbon substrates (Choreño-Parra and Treseder 2024; Shao et al. 2023).

Consistent with these enzymatic constraints, the carbon quality index declined under ECM inoculation, especially within the hyphosphere, indicating a shift in microbial substrate use away from readily decomposable carbon. Rather than reflecting reduced microbial activity, this lower CQI suggests a strategic redirection of carbon processing away from rapid mineralization and toward pathways favoring structural retention and longer residence times (Frey et al.

2004; Terrer et al. 2019). Collectively, these findings demonstrate that although N enrichment alone promotes microbial investment in oxidative decomposition, ECM fungi override this response by suppressing key enzymatic functions, thereby redirecting carbon fluxes toward more conservative processing routes and reshaping SOC stabilization trajectories under N enrichment (Frey et al. 2004; Phillips et al. 2013).

ECM-mediated restructuring of microbial communities and functional potential

Building on ECM-driven shifts in enzyme investment strategies, concurrent changes in microbial community structure and functional potential provide a critical biological basis for the reorganization of soil carbon processing pathways (Schimel and Schaeffer 2012; Malik et al. 2020). N addition and ECM inoculation acted interactively to reshape microbial composition, diversity, and functional traits, thereby regulating how carbon inputs were transformed, partitioned, and retained in soil (Phillips et al. 2013; Maynard et al. 2017).

Consistent with ECM-dominated forest soils, bacterial communities numerically dominated the microbiome, whereas fungal communities, despite lower relative abundance, were more sensitive to both N availability and ECM presence. N addition reduced microbial α-diversity in a U-shaped manner, with minimum diversity at intermediate N levels, suggesting initial suppression of sensitive taxa followed by community restructuring under higher N inputs (Ramirez et al. 2012). ECM inoculation further modified these trajectories by dampening compositional divergence and promoting functional convergence under elevated N conditions, consistent with ECM-mediated buffering of microbial responses (Averill et al. 2014).

Community–environment linkages revealed clear functional differentiation between bacteria and fungi (Li et al. 2026). Bacterial composition was primarily structured by labile carbon-related variables and hydrolytic enzyme activities, including S-β-GC, DOC, and CQI, underscoring tight coupling to short-term carbon turnover (Allison et al. 2014; Kielak et al. 2016). In contrast, fungal communities were more strongly associated with indicators of carbon stabilization, including MAOC, SOC chemical properties, and inorganic N forms, reinforcing the role of fungi, particularly under ECM influence, in regulating longer-term SOC persistence (Six et al. 2006; Clemmensen et al. 2013).

The regulatory importance of microbial communities was further supported by integrative analyses. Correlation analyses linked fungal abundance to hydrolytic enzyme activities, microbial necromass accumulation, and N availability, highlighting fungi as key mediators connecting nutrient inputs to carbon transformation pathways (Xu et al. 2024; Cheng et al. 2025). Random forest models similarly indicated that SOC dynamics were driven by a limited set of bacterial and fungal taxa rather than by overall diversity, emphasizing functional identity over taxonomic richness. Notably, several ECM-associated or saprotrophic fungi, including *Penicillium*, *Thelephora*, and *Trichoderma*, emerged as dominant regulators of soil carbon pools, underscoring the primacy of fungal functional traits in SOC stabilization (Domeignoz-Horta et al. 2021).

At the functional gene level, CAZy profiling showed that plant-derived carbohydrate-active enzymes dominated across all carbon pools, reflecting the central role of plant inputs as substrates for soil carbon transformation. However, their frequent negative associations with SOC, DOC, and MAOC accumulation suggest that intensified depolymerization may accelerate carbon loss rather than stabilization (Ren et al. 2021; Xiong et al. 2023). In contrast, a small subset of microbial-derived enzymes, particularly bacterial GH104 and fungal GH17, exhibited consistent, pool-specific regulatory roles across DOC, POC, MAOC, and MBC, pointing to functional redundancy among plant-associated enzymes and high-leverage, niche-specific effects of select microbial functions (Dai et al. 2021).

The inverse relationships between enzymatic potential and carbon accumulation align with widespread enzyme suppression under ECM inoculation and broader evidence linking CAZy functional potential to ecosystem carbon dynamics (Xiong et al. 2023). Together, these findings indicate that ECM fungi restructure microbial communities and functional potential in ways that constrain excessive enzymatic degradation and reinforce carbon retention pathways, establishing a microbial framework favoring moderated decomposition and enhanced necromass contributions to stable SOC pools (Ren et al. 2021; Xiong et al. 2023).

Microbial necromass as a dominant pathway for SOC persistence

Growing evidence indicates that SOC persistence is governed less by intrinsic chemical recalcitrance than by biologically mediated stabilization processes (Qiao et al. 2025). Consistent with this paradigm, our integrative analyses identify microbial necromass formation, rather than substrate chemical resistance, as the dominant pathway regulating SOC stabilization under combined N addition and ECM inoculation (Cotrufo et al. 2013; Liang et al. 2017). Among all microbial-derived indices, FNC and MCP efficiency showed the strongest sensitivity to the N × ECM interaction, indicating that ECM fungi fundamentally reprogram microbial carbon processing under N enrichment (Sokol et al. 2019; Malik et al. 2020). This responsiveness reflects a mechanistic shift away from decomposition-driven carbon turnover toward necromass-mediated carbon retention.

This shift is reinforced by pronounced spatial differentiation between the hyphosphere and the mycorrhizosphere. Higher FNC accumulation and MCP efficiency in the hyphosphere suggest that ECM extraradical mycelia create microhabitats favoring rapid microbial biomass turnover coupled with enhanced necromass preservation, likely through constrained enzyme investment and altered nutrient accessibility (Clemmensen et al. 2013; Averill and Hawkes 2016). Such spatial decoupling implies that ECM fungi regulate SOC stabilization through localized control over microbial activity and carbon fate rather than as a uniform bulk-soil process.

In contrast, lignin-derived indicators responded weakly and inconsistently to both N addition and ECM inoculation and did not emerge as dominant predictors of SOC pool variation in multivariate or machine-learning analyses. This limited explanatory power suggests that selective preservation of chemically recalcitrant plant residues plays a secondary role in SOC stabilization under these conditions relative to biologically mediated pathways (Schmidt et al. 2011; Lehmann and Kleber 2015).

Consistent with this interpretation, MAOC accumulation aligned more closely with MCP-related indices than with NMR-derived measures of SOC hydrophobicity or chemical inertness (Cotrufo et al. 2013; Liang et al. 2017). Although N addition increased SOC hydrophobicity, this chemical shift did not translate into enhanced MAOC formation, highlighting a decoupling between chemical composition and carbon persistence (Lehmann and Kleber 2015; Schmidt et al. 2011). Instead, MAOC dynamics tracked microbial necromass-related metrics, indicating that mineral-associated carbon formation was primarily governed by microbial turnover and residue stabilization rather than increased chemical resistance (Sokol et al. 2019; Kallenbach et al. 2015).

Taken together, these results demonstrate that under N enrichment, ECM fungi redirect SOC stabilization away from chemistry-driven persistence toward microbial necromass-dominated mechanisms characterized by strong spatial structuring and limited involvement of lignin chemistry (Averill and Hawkes 2016; Clemmensen et al. 2013). This decoupling challenges traditional paradigms of carbon persistence and underscores the central role of microbial carbon pumping in ECM-dominated forest soils (Liang et al. 2017; Malik et al. 2020).

Implications for forest soil carbon sequestration under changing N regimes

Our results demonstrate that ECM fungi act as critical biotic regulators of soil carbon sequestration strength and stability under increasing N deposition. Rather than exerting uniform effects, N enrichment altered SOC pools and stabilization pathways in a manner strongly contingent on ECM presence, highlighting the central role of biological mediation in forest soil carbon responses to global change (Averill and Hawkes 2016; Clemmensen et al. 2013).

Across the N gradient, increased N availability did not necessarily enhance SOC stability. Although N addition promoted shifts toward chemically more hydrophobic SOC, these changes did not translate into consistent increases in MAOC. Instead, SOC persistence depended primarily on how N reshaped microbial carbon processing pathways and necromass formation rather than increased chemical recalcitrance alone, challenging the assumption that N deposition universally strengthens soil carbon sinks (Schmidt et al. 2011; Lehmann and Kleber 2015).

Within this context, ECM fungi played a decisive role in determining SOC stabilization pathways under N enrichment. By suppressing oxidative enzyme activity and restructuring microbial community composition and enzyme investment, ECM fungi redirected carbon fluxes away from rapid mineralization toward microbial necromass accumulation and subsequent mineral association. This ECM-mediated regulation of the microbial carbon pump indicates that SOC persistence is governed less by substrate chemistry per se than by biologically controlled carbon processing and turnover pathways (Cotrufo et al. 2013; Averill et al. 2014; Liang et al. 2017).

These mechanisms have direct implications for carbon management in plantation forests, particularly fast-growing systems such as *Eucalyptus*. N fertilization or elevated atmospheric N deposition may enhance aboveground productivity without proportionally increasing long-term soil carbon storage if ECM-mediated necromass pathways are weakened or disrupted. Management strategies that overlook mycorrhizal functioning may therefore overestimate carbon sequestration potential under high N inputs (Phillips et al. 2013; Terrer et al. 2019).

More broadly, our findings underscore the need to explicitly incorporate microbial and mycorrhizal controls into SOC stabilization parameterization in Earth system and ecosystem models. Current frameworks often emphasize chemical recalcitrance or bulk SOC pools, whereas our results demonstrate that microbial necromass formation, enzyme allocation strategies, and mycorrhizal regulation are key determinants of SOC persistence under changing N regimes. Incorporating ECM-mediated microbial carbon pump processes will be essential for improving predictions of forest soil carbon dynamics in a high-N world (Wieder et al. 2015; Malik et al. 2020).

Taken together, our results highlight ECM fungi as central biotic regulators of soil carbon persistence under N enrichment. By modulating microbial enzyme investment, community composition, and necromass formation, ECM fungi redirect carbon from fast-turnover pools into mineral-associated fractions, decoupling SOC stabilization from

chemical recalcitrance. These findings emphasize that biologically mediated processes, rather than substrate chemistry alone, govern long-term SOC dynamics in ECM-dominated forests. Incorporating microbial and mycorrhizal controls into forest carbon models is therefore critical for accurately predicting soil carbon responses to global change.

Open Access This article is licensed under a Creative Commons Attribution 4.0 International License, which permits use, sharing, adaptation, distribution and reproduction in any medium or format, as long as you give appropriate credit to the original author(s) and the source, provide a link to the Creative Commons licence, and indicate if changes were made. The images or other third party material in this article are included in the article's Creative Commons licence, unless indicated otherwise in a credit line to the material. If material is not included in the article's Creative Commons licence and your intended use is not permitted by statutory regulation or exceeds the permitted use, you will need to obtain permission directly from the copyright holder. To view a copy of this licence, visit http://creativecommons.org/licenses/by/4.0/.

References

Allison SD, Vitousek PM (2005) Responses of extracellular enzymes to simple and complex nutrient inputs. Soil Biol Biochem 37(5):937–944. https://doi.org/10.1016/j.soilbio.2004.09.014

Averill C, Hawkes CV (2016) Ectomycorrhizal fungi slow soil carbon cycling. Ecol Lett 19(8):937–947. https://doi.org/10.1111/ele.12631

Averill C, Turner BL, Finzi AC (2014) Mycorrhiza-mediated competition between plants and decomposers drives soil carbon storage. Nature 505(7484):543–545. https://doi.org/10.1038/nature12901

Bååth E, Nilsson LO, Göransson H, Wallander H (2004) Can the extent of degradation of soil fungal *mycelium* during soil incubation be used to estimate ectomycorrhizal biomass in soil? Soil Biol Biochem 36(12):2105–2109. https://doi.org/10.1016/j.soilbio.2004.06.004

Bera T, Vardanyan L, Inglett KS, Reddy KR, O'Connor GA, Erickson JE, Wilkie AC (2019) Influence of select bioenergy by-products on soil carbon and microbial activity: a laboratory study. Sci Total Environ 653:1354–1363. https://doi.org/10.1016/j.scitotenv.2018.10.237

Bödeker ITM, Clemmensen KE, de Boer W, Martin F, Olson Å, Lindahl BD (2014) Ectomycorrhizal *Cortinarius* species participate in enzymatic oxidation of humus in northern forest ecosystems. New Phytol 203(1):245–256. https://doi.org/10.1111/nph.12791

Buchfink B, Xie C, Huson DH (2015) Fast and sensitive protein alignment using DIAMOND. Nat Methods 12(1):59–60. https://doi.org/10.1038/nmeth.3176

Cantarel BL, Coutinho PM, Rancurel C, Bernard T, Lombard V, Henrissat B (2009) The carbohydrate-active EnZymes database (CAZy): an expert resource for glycogenomics. Nucleic Acids Res 37:D233–D238. https://doi.org/10.1093/nar/gkn663

Chen J, Elsgaard L, van Groenigen KJ, Olesen JE, Liang Z, Jiang Y, Lærke PE, Zhang YF, Luo YQ, Hungate BA, Sinsabaugh RL, Jørgensen U (2020) Soil carbon loss with warming: new evidence from carbon-degrading enzymes. Glob Change Biol 26(4):1944–1952. https://doi.org/10.1111/gcb.14986

Chen SG, Zhang YQ, Ma J, Bai MY, Long JX, Liu M, Chen YL, Guo JB, Chen L (2025a) Contribution of soil microbial necromass carbon to soil organic carbon fractions and its influencing factors in different grassland types. Soil 11(2):883–898. https://doi.org/10.5194/soil-11-883-2025

Chen X, Cao JJ, Sinsabaugh RL, Moorhead DL, Bardgett RD, Fanin N, Nottingham AT, Zheng XH, Chen J (2025b) Soil extracellular enzymes as drivers of soil carbon storage under nitrogen addition. Biol Rev 100(4):1716–1733. https://doi.org/10.1111/brv.70021

Cheng YD, Huang JJ, Wang SL, Xiong K, Liang K, Wang FC, Wang SN, Zhang HP, Wang GG, Chen FS (2025) Exploring the boost by dominant ectomycorrhizal trees to soil organic carbon sequestration in the subtropical forest of the Jiulianshan National Nature Reserve. J for Res 36(1):131. https://doi.org/10.1007/s11676-025-01924-w

Choreño-Parra EM, Treseder KK (2024) Mycorrhizal fungi modify decomposition: a meta-analysis. New Phytol 242(6):2763–2774. https://doi.org/10.1111/nph.19748

Clemmensen KE, Bahr A, Ovaskainen O, Dahlberg A, Ekblad A, Wallander H, Stenlid J, Finlay RD, Wardle DA, Lindahl BD (2013) Roots and associated fungi drive long-term carbon sequestration in boreal forest. Science 339(6127):1615–1618. https://doi.org/10.1126/science.1231923

Cotillard A, Kennedy SP, Kong LC, Prifti E, Pons N, Le Chatelier E, Almeida M, Quinquis B, Levenez F, Galleron N, Gougis S, Rizkalla S, Batto JM, Renault P, Doré J, Zucker JD, Clément K, Ehrlich SD (2013) Dietary intervention impact on gut microbial gene richness. Nature 500(7464):585–588. https://doi.org/10.1038/nature12480

Cotrufo MF, Wallenstein MD, Boot CM, Denef K, Paul E (2013) The Microbial Efficiency-Matrix Stabilization (MEMS) framework integrates plant litter decomposition with soil organic matter stabilization: do labile plant inputs form stable soil organic matter? Glob Change Biol 19(4):988–995. https://doi.org/10.1111/gcb.12113

Cotrufo MF, Soong JL, Horton AJ, Campbell EE, Haddix ML, Wall DH, Parton WJ (2015) Formation of soil organic matter *via* biochemical and physical pathways of litter mass loss. Nat Geosci 8(10):776–779. https://doi.org/10.1038/ngeo2520

Dai ZM, Zang HD, Chen J, Fu YY, Wang XH, Liu HT, Shen CC, Wang JJ, Kuzyakov Y, Becker JN, Hemp A, Barberán A, Gunina A, Chen HH, Luo Y, Xu JM (2021) Metagenomic insights into soil microbial communities involved in carbon cycling along an elevation climosequences. Environ Microbiol 23(8):4631–4645. https://doi.org/10.1111/1462-2920.15655

Domeignoz-Horta LA, Shinfuku M, Junier P, Poirier S, Verrecchia E, Sebag D, DeAngelis KM (2021) Direct evidence for the role of microbial community composition in the formation of soil organic matter composition and persistence. ISME Commun 1(1):64. https://doi.org/10.1038/s43705-021-00071-7

Fang YY, Nazaries L, Singh BK, Singh BP (2018) Microbial mechanisms of carbon priming effects revealed during the interaction of crop residue and nutrient inputs in contrasting soils. Glob Change Biol 24(7):2775–2790. https://doi.org/10.1111/gcb.14154

Feng Q, Liang SS, Jia HJ, Stadlmayr A, Tang LQ, Lan Z, Zhang DY, Xia HH, Xu XY, Jie ZY, Su LL, Li XP, Li X, Li JH, Xiao L, Huber-Schönauer U, Niederseer D, Xu X, Al-Aama JY, Yang HM, Wang J, Kristiansen K, Arumugam M, Tilg H, Datz C, Wang J (2015) Gut microbiome development along the colorectal adenoma–carcinoma sequence. Nat Commun 6:6528. https://doi.org/10.1038/ncomms7528

Frey SD, Knorr M, Parrent JL, Simpson RT (2004) Chronic nitrogen enrichment affects the structure and function of the soil microbial community in temperate hardwood and pine forests. For Ecol Manag 196(1):159–171. https://doi.org/10.1016/j.foreco.2004.03.018

Frey SD, Ollinger S, Nadelhoffer K, Bowden R, Brzostek E, Burton A, Caldwell BA, Crow S, Goodale CL, Grandy AS, Finzi A, Kramer MG, Lajtha K, LeMoine J, Martin M, McDowell WH, Minocha R, Sadowsky JJ, Templer PH, Wickings K (2014) Chronic nitrogen additions suppress decomposition and sequester soil carbon in

temperate forests. Biogeochemistry 121(2):305–316. https://doi.org/10.1007/s10533-014-0004-0

Galloway JN, Townsend AR, Erisman JW, Bekunda M, Cai ZC, Freney JR, Martinelli LA, Seitzinger SP, Sutton MA (2008) Transformation of the nitrogen cycle: recent trends, questions, and potential solutions. Science 320(5878):889–892. https://doi.org/10.1126/science.1136674

Geng PF, Jin GZ (2022) Fine root morphology and chemical responses to N addition depend on root function and soil depth in a Korean pine plantation in Northeast China. For Ecol Manag 520:120407. https://doi.org/10.1016/j.foreco.2022.120407

Guan X, Jiang J, Classen AT, Ullah S, Wang GS (2025) Disentangling the contribution of mycorrhizal fungi to soil organic carbon storage. Soil Biol Biochem 209:109900. https://doi.org/10.1016/j.soilbio.2025.109900

He WY, Wei HJ, Liang JW, Xu TY, Chen H, Hu WT, Tang M (2024) How do ectomycorrhizal fungi regulate *Eucalyptus* biomass allocation through the stoichiometric changes in the plant-soil-microbe system under nitrogen addition? Ind Crops Prod 218:118876. https://doi.org/10.1016/j.indcrop.2024.118876

He WY, Zhang MM, Jin GZ, Sui X, Zhang T, Song FQ (2021) Effects of nitrogen deposition on nitrogen-mineralizing enzyme activity and soil microbial community structure in a Korean pine plantation. Microb Ecol 81(2):410–424. https://doi.org/10.1007/s00248-020-01595-6

Hendricks JJ, Mitchell RJ, Kuehn KA, Pecot SD (2016) Ectomycorrhizal fungal mycelia turnover in a longleaf pine forest. New Phytol 209:1693–1704

Hu JX, Huang CD, Zhou SX, Liu X, Dijkstra FA (2022) Nitrogen addition increases microbial necromass in croplands and bacterial necromass in forests: a global meta-analysis. Soil Biol Biochem 165:108500. https://doi.org/10.1016/j.soilbio.2021.108500

Hu YL, Chen J, Olesen JE, van Groenigen KJ, Hui DF, He XH, Chen GY, Deng Q (2024) Mycorrhizal association controls soil carbon-degrading enzyme activities and soil carbon dynamics under nitrogen addition: a systematic review. Sci Total Environ 948:175008. https://doi.org/10.1016/j.scitotenv.2024.175008

Huson DH, Mitra S, Ruscheweyh HJ, Weber N, Schuster SC (2011) Integrative analysis of environmental sequences using MEGAN4. Genome Res 21(9):1552–1560. https://doi.org/10.1101/gr.120618.111

Kallenbach CM, Grandy AS, Frey SD, Diefendorf AF (2015) Microbial physiology and necromass regulate agricultural soil carbon accumulation. Soil Biol Biochem 91:279–290. https://doi.org/10.1016/j.soilbio.2015.09.005

Karlsson FH, Tremaroli V, Nookaew I, Bergström G, Behre CJ, Fagerberg B, Nielsen J, Bäckhed F (2013) Gut metagenome in European women with normal, impaired and diabetic glucose control. Nature 498(7452):99–103. https://doi.org/10.1038/nature12198

Kielak AM, Barreto CC, Kowalchuk GA, van Veen JA, Kuramae EE (2016) The ecology of acidobacteria: moving beyond genes and genomes. Front Microbiol 7:744. https://doi.org/10.3389/fmicb.2016.00744

Lehmann J, Kleber M (2015) The contentious nature of soil organic matter. Nature 528(7580):60–68. https://doi.org/10.1038/nature16069

Lehmann J, Hansel CM, Kaiser C, Kleber M, Maher K, Manzoni S, Nunan N, Reichstein M, Schimel JP, Torn MS, Wieder WR, Kögel-Knabner I (2020) Persistence of soil organic carbon caused by functional complexity. Nat Geosci 13(8):529–534. https://doi.org/10.1038/s41561-020-0612-3

Li JH, Jia HJ, Cai XH, Zhong HZ, Feng Q, Sunagawa S, Arumugam M, Kultima JR, Prifti E, Nielsen T, Juncker AS, Manichanh C, Chen B, Zhang WW, Levenez F, Wang J, Xu X, Xiao L, Liang SS, Zhang DY, Zhang ZX, Chen WN, Zhao HL, Al-Aama JY, Edris S, Yang HM, Wang J, Hansen T, Nielsen HB, Brunak S, Kristiansen K, Guarner F, Pedersen O, Doré J, Ehrlich SD, Bork P, Wang J (2014) An integrated catalog of reference genes in the human gut microbiome. Nat Biotechnol 32(8):834–841. https://doi.org/10.1038/nbt.2942

Li J, Liu Y, Chen S, Zhou D, Zhang H, Wang J, Li H, Ren Y, Wang C, Song H, Yang X (2026) Soil bacteria drive the pattern of tree regeneration by mediating spatial variation of soil nutrients. J for Res 37:55. https://doi.org/10.1007/s11676-026-01994-4

Liang C, Amelung W, Lehmann J, Kästner M (2019) Quantitative assessment of microbial necromass contribution to soil organic matter. Glob Change Biol 25(11):3578–3590. https://doi.org/10.1111/gcb.14781

Liang C, Balser TC (2012) Warming and nitrogen deposition lessen microbial residue contribution to soil carbon pool. Nat Commun 3:1222. https://doi.org/10.1038/ncomms2224

Liang C, Schimel JP, Jastrow JD (2017) The importance of anabolism in microbial control over soil carbon storage. Nat Microbiol 2:17105. https://doi.org/10.1038/nmicrobiol.2017.105

Lindahl BD, Tunlid A (2015) Ectomycorrhizal fungi–potential organic matter decomposers, yet not saprotrophs. New Phytol 205(4):1443–1447. https://doi.org/10.1111/nph.13201

Liu L, Wen Z, Liu S, Zhang XY, Liu XJ (2024) Decline in atmospheric nitrogen deposition in China between 2010 and 2020. Nat Geosci 17(8):733–736. https://doi.org/10.1038/s41561-024-01484-4

Liu L, Yang JJ, Wang J, Yu Q, Wei CZ, Jiang LC, Huang JH, Zhang YH, Jiang Y, Zhang HY, Han XG (2025) Increase in mineral-associated organic carbon does not offset the decrease in particulate organic carbon under long-term nitrogen enrichment in a steppe ecosystem. Soil Biol Biochem 202:109695. https://doi.org/10.1016/j.soilbio.2024.109695

Lu XF, Hou EQ, Guo JY, Gilliam FS, Li JL, Tang SB, Kuang YW (2021) Nitrogen addition stimulates soil aggregation and enhances carbon storage in terrestrial ecosystems of China: a meta-analysis. Glob Change Biol 27(12):2780–2792. https://doi.org/10.1111/gcb.15604

Ma T, Zhu SS, Wang ZH, Chen DM, Dai GH, Feng BW, Su XY, Hu HF, Li KH, Han WX, Liang C, Bai YF, Feng XJ (2018) Divergent accumulation of microbial necromass and plant lignin components in grassland soils. Nat Commun 9:3480. https://doi.org/10.1038/s41467-018-05891-1

Malik AA, Martiny JBH, Brodie EL, Martiny AC, Treseder KK, Allison SD (2020) Defining trait-based microbial strategies with consequences for soil carbon cycling under climate change. ISME J 14(1):1–9. https://doi.org/10.1038/s41396-019-0510-0

Maynard DS, Crowther TW, Bradford MA (2017) Fungal interactions reduce carbon use efficiency. Ecol Lett 20(8):1034–1042. https://doi.org/10.1111/ele.12801

Mielke LA, Klein J, Ekblad A, Finlay RD, Lindahl BD, Clemmensen KE (2025) Fungal guild interactions slow decomposition of boreal forest pine litter and humus. New Phytol 247(5):2367–2380. https://doi.org/10.1111/nph.70316

Phillips RP, Brzostek E, Midgley MG (2013) The mycorrhizal-associated nutrient economy: a new framework for predicting carbon–nutrient couplings in temperate forests. New Phytol 199(1):41–51. https://doi.org/10.1111/nph.12221

Plett KL, Wojtalewicz D, Anderson IC, Plett JM (2024) Fungal metabolism and free amino acid content may predict nitrogen transfer to the host plant in the ectomycorrhizal relationship between *Pisolithus* spp. and *Eucalyptus grandis*. New Phytol 242(4):1589–1602. https://doi.org/10.1111/nph.19400

Qiao LK, Wang JF, Wei SS, Ren YL, Lichtfouse E, Han J (2025) The soil microbial carbon pump for carbon sequestration. Environ Chem Lett 23(5):1145–1151. https://doi.org/10.1007/s10311-025-01861-4

Qin JJ, Li RQ, Raes J, Arumugam M, Burgdorf KS, Manichanh C, Nielsen T, Pons N, Levenez F, Yamada T, Mende DR, Li JH, Xu JM, Li SC, Li DF, Cao JJ, Wang B, Liang HQ, Zheng HS, Xie YL, Tap J, Lepage P, Bertalan M, Batto JM, Hansen T, Le Paslier D, Linneberg A, Nielsen HB, Pelletier E, Renault P, Sicheritz-Ponten T, Turner K, Zhu HM, Yu C, Li ST, Jian M, Zhou Y, Li YR, Zhang XQ, Li SG, Qin N, Yang HM, Wang J, Brunak S, Doré J, Guarner F, Kristiansen K, Pedersen O, Parkhill J, Weissenbach J, Bork P, Ehrlich SD, Wang J (2010) A human gut microbial gene catalogue established by metagenomic sequencing. Nature 464(7285):59–65. https://doi.org/10.1038/nature08821

Qin N, Yang FL, Li A, Prifti E, Chen YF, Shao L, Guo J, Le Chatelier E, Yao J, Wu LJ, Zhou JW, Ni SJ, Liu L, Pons N, Batto JM, Kennedy SP, Leonard P, Yuan CH, Ding WC, Chen YT, Hu XJ, Zheng BW, Qian GR, Xu W, Ehrlich SD, Zheng SS, Li LJ (2014) Alterations of the human gut microbiome in liver cirrhosis. Nature 513(7516):59–64. https://doi.org/10.1038/nature13568

Ramirez KS, Craine JM, Fierer N (2012) Consistent effects of nitrogen amendments on soil microbial communities and processes across biomes. Glob Change Biol 18(6):1918–1927. https://doi.org/10.1111/j.1365-2486.2012.02639.x

Reay DS, Dentener F, Smith P, Grace J, Feely RA (2008) Global nitrogen deposition and carbon sinks. Nat Geosci 1(7):430–437. https://doi.org/10.1038/ngeo230

Ren CJ, Zhang XY, Zhang SH, Wang JY, Xu MP, Guo YX, Wang J, Han XH, Zhao FZ, Yang GH, Doughty R (2021) Altered microbial CAZyme families indicated dead biomass decomposition following afforestation. Soil Biol Biochem 160:108362. https://doi.org/10.1016/j.soilbio.2021.108362

Schimel JP, Schaeffer SM (2012) Microbial control over carbon cycling in soil. Front Microbio 3:348. https://doi.org/10.3389/fmicb.2012.00348

Schmidt MWI, Torn MS, Abiven S, Dittmar T, Guggenberger G, Janssens IA, Kleber M, Kögel-Knabner I, Lehmann J, Manning DAC, Nannipieri P, Rasse DP, Weiner S, Trumbore SE (2011) Persistence of soil organic matter as an ecosystem property. Nature 478(7367):49–56. https://doi.org/10.1038/nature10386

Shao SY, Wurzburger N, Sulman B, Hicks Pries C (2023) Ectomycorrhizal effects on decomposition are highly dependent on fungal traits, climate, and litter properties: a model-based assessment. Soil Biol Biochem 184:109073. https://doi.org/10.1016/j.soilbio.2023.109073

Sinsabaugh RL (2010) Phenol oxidase, peroxidase and organic matter dynamics of soil. Soil Biol Biochem 42(3):391–404. https://doi.org/10.1016/j.soilbio.2009.10.014

Six J, Frey SD, Thiet RK, Batten KM (2006) Bacterial and fungal contributions to carbon sequestration in agroecosystems. Soil Sci Soc Am J 70(2):555–569. https://doi.org/10.2136/sssaj2004.0347

Smith S, Read DJ (2008) Mycorrhizal symbiosis, third ed. Academic Press, London

Sokol NW, Sanderman J, Bradford MA (2019) Pathways of mineral-associated soil organic matter formation: integrating the role of plant carbon source, chemistry, and point of entry. Glob Change Biol 25(1):12–24. https://doi.org/10.1111/gcb.14482

Stevens CJ, Dise NB, Mountford JO, Gowing DJ (2004) Impact of nitrogen deposition on the species richness of grasslands. Science 303(5665):1876–1879

Sunagawa S, Coelho LP, Chaffron S, Kultima JR, Labadie K, Salazar G, Djahanschiri B, Zeller G, Mende DR, Alberti A, Cornejo-Castillo FM, Costea PI, Cruaud C, D'Ovidio F, Engelen S, Ferrera I, Gasol JM, Guidi L, Hildebrand F, Kokoszka F, Lepoivre C, Lima-Mendez G, Poulain J, Poulos BT, Royo-Llonch M, Sarmento H, Vieira-Silva S, Dimier C, Picheral M, Searson S, Kandels-Lewis S, Bowler C, de Vargas C, Gorsky G, Grimsley N, Hingamp P, Iudicone D, Jaillon O, Not F, Ogata H, Pesant S, Speich S, Stemmann L, Sullivan MB, Weissenbach J, Wincker P, Karsenti E, Raes J, Acinas SG, Bork P, Boss E, Bowler C, Follows M, Karp-Boss L, Krzic U, Reynaud EG, Sardet S, Sieracki S, Velayoudon D (2015) Structure and function of the global ocean microbiome. Science 348(6237):1261359. https://doi.org/10.1126/science.1261359

Terrer C, Jackson RB, Prentice IC, Keenan TF, Kaiser C, Vicca S, Fisher JB, Reich PB, Stocker BD, Hungate BA, Peñuelas J, McCallum I, Soudzilovskaia NA, Cernusak LA, Talhelm AF, Van Sundert K, Piao SL, Newton PCD, Hovenden MJ, Blumenthal DM, Liu YY, Müller C, Winter K, Field CB, Viechtbauer W, Van Lissa CJ, Hoosbeek MR, Watanabe M, Koike T, Leshyk VO, Polley HW, Franklin O (2019) Nitrogen and phosphorus constrain the CO_2 fertilization of global plant biomass. Nat Clim Change 9(9):684–689. https://doi.org/10.1038/s41558-019-0545-2

Tian J, Dungait JAJ, Lu XK, Yang YF, Hartley IP, Zhang W, Mo JM, Yu GR, Zhou JZ, Kuzyakov Y (2019) Long-term nitrogen addition modifies microbial composition and functions for slow carbon cycling and increased sequestration in tropical forest soil. Glob Change Biol 25(10):3267–3281. https://doi.org/10.1111/gcb.14750

Ullah MR, Carrillo Y, Dijkstra FA (2021) Drought-induced and seasonal variation in carbon use efficiency is associated with fungi: bacteria ratio and enzyme production in a grassland ecosystem. Soil Biol Biochem 155:108159. https://doi.org/10.1016/j.soilbio.2021.108159

Visscher AM, Vanek S, Meza K, de Goede RGM, Valverde AA, Ccanto R, Olivera E, Scurrah M, Fonte SJ (2020) *Eucalyptus* and alder field margins differ in their impact on ecosystem services and biodiversity within cropping fields of the Peruvian *Andes*. Agric Ecosyst Environ 303:107107. https://doi.org/10.1016/j.agee.2020.107107

Wang BR, An SS, Liang C, Liu Y, Kuzyakov Y (2021) Microbial necromass as the source of soil organic carbon in global ecosystems. Soil Biol Biochem 162:108422. https://doi.org/10.1016/j.soilbio.2021.108422

Wang Z, Yang L, Wang J, Zhao X, Zhang C, von Gadow K (2025) Soil fertility and forest structure influence tree carbon stock depending on mycorrhizal types in a temperate forest. J for Res 36:115. https://doi.org/10.1007/s11676-025-01908-w

Wieder WR, Allison SD, Davidson EA, Georgiou K, Hararuk O, He YJ, Hopkins F, Luo YQ, Smith MJ, Sulman B, Todd-Brown K, Wang YP, Xia JY, Xu XF (2015) Explicitly representing soil microbial processes in Earth system models. Glob Biogeochem Cycles 29(10):1782–1800. https://doi.org/10.1002/2015GB005188

Willard SJ, Vanguelova E, Waring B (2026) Nitrogen deposition is linked to changes in mineral-associated organic carbon in forest soils in the United Kingdom. Plant Soil 519(2):2051–2069. https://doi.org/10.1007/s11104-025-08268-8

Wu H, Yang JJ, Fu W, Rillig MC, Cao ZJ, Zhao AH, Hao ZP, Zhang X, Chen BD, Han XG (2023a) Identifying thresholds of nitrogen enrichment for substantial shifts in arbuscular mycorrhizal fungal community metrics in a temperate grassland of Northern China. New Phytol 237(1):279–294. https://doi.org/10.1111/nph.18516

Wu JJ, Zhang H, Pan YT, Cheng XL, Zhang KR, Liu GH (2023b) Particulate organic carbon is more sensitive to nitrogen addition than mineral-associated organic carbon: a meta-analysis. Soil Tillage Res 232:105770. https://doi.org/10.1016/j.still.2023.105770

Wu R, Zhang H, Zhang M, Jin G, Song F (2025) Saprotrophic fungal community responses to nitrogen additions in a Korean pine plantation: insights from using the mycoindicator. J for Res 36:27. https://doi.org/10.1007/s11676-025-01821-2

Xiong MY, Jiang W, Zou SZ, Kang D, Yan XC (2023) Microbial carbohydrate-active enzymes influence soil carbon by regulating the of plant- and fungal-derived biomass decomposition in plateau

peat wetlands under differing water conditions. Front Microbiol 14:1266016. https://doi.org/10.3389/fmicb.2023.1266016

Xu FD, Li C, Chen YX, Wu JC, Bai HD, Fan SG, Yang YC, Zhang YP, Li SF, Su JR (2024) Soil microbial community structure and soil fertility jointly regulate soil microbial residue carbon during the conversion from subtropical primary forest to plantations. Geoderma 441:116767. https://doi.org/10.1016/j.geoderma.2023.116767

Xu JR, Zhu WL, Yu SH, Dun XJ, Hu DM, Liao DX, Hao M, Lian FJ, Zhang ZX, Gao P (2025) Effects of thinning on soil microbial community and carbon fractions and their relationships in coastal protected forests. Environ Earth Sci 84(8):207. https://doi.org/10.1007/s12665-025-12202-7

Yang LY, Canarini A, Zhang WS, Lang M, Chen YX, Cui ZL, Kuzyakov Y, Richter A, Chen XP, Zhang FS, Tian J (2024) Microbial life-history strategies mediate microbial carbon pump efficacy in response to N management depending on stoichiometry of microbial demand. Glob Change Biol 30(5):e17311. https://doi.org/10.1111/gcb.17311

Yu GR, Jia YL, He NP, Zhu JX, Chen Z, Wang QF, Piao SL, Liu XJ, He HL, Guo XB, Wen Z, Li P, Ding GA, Goulding K (2019) Stabilization of atmospheric nitrogen deposition in China over the past decade. Nat Geosci 12(6):424–429. https://doi.org/10.1038/s41561-019-0352-4

Yu YL, Zhu NX, Ren Y, Dong MH, Sun GF, Virk AL, Li FM, Yang HS, Kan ZR (2025) Effects of crop rotation on plant- and microbial-derived carbon within particulate and mineral fractions in paddy soils. Agric Ecosyst Environ 380:109398. https://doi.org/10.1016/j.agee.2024.109398

Yuan X, Qin WK, Xu H, Zhang ZH, Zhou HK, Zhu B (2020) Sensitivity of soil carbon dynamics to nitrogen and phosphorus enrichment in an Alpine meadow. Soil Biol Biochem 150:107984. https://doi.org/10.1016/j.soilbio.2020.107984

Zhang MM, Lu Y, Jin GZ, Zhu B (2026) Bacterial communities in litter are more sensitive to high nitrogen addition than fungal communities in a Korean pine (*Pinus koraiensis*) plantation. J For Res 37(1):23. https://doi.org/10.1007/s11676-025-01961-5

Zhang XY, Jia J, Chen LT, Chu HY, He JS, Zhang YJ, Feng XJ (2021) Aridity and NPP constrain contribution of microbial necromass to soil organic carbon in the Qinghai-Tibet Alpine grasslands. Soil Biol Biochem 156:108213. https://doi.org/10.1016/j.soilbio.2021.108213

Zhu XF, Jackson RD, DeLucia EH, Tiedje JM, Liang C (2020) The soil microbial carbon pump: from conceptual insights to empirical assessments. Glob Change Biol 26(11):6032–6039. https://doi.org/10.1111/gcb.15319

Publisher's Note Springer Nature remains neutral with regard to jurisdictional claims in published maps and institutional affiliations.